NAVAL POSTGRADUATE SCHOOL

MONTEREY, CALIFORNIA

THESIS

COMPARISON OF POLARIRIMETRIC CAMERAS

by

Jarrad A. Smoke

March 2017

Thesis Advisor: R.C. Olsen
Co-Advisor: D. Trask

Approved for public release. Distribution is unlimited.

THIS PAGE INTENTIONALLY LEFT BLANK

REPORT DOCUMENTATION PAGE			Form Approved OMB No. 0704-0188
Public reporting burden for this collection of information is estimated to average 1 hour per response, including the time for reviewing instruction, searching existing data sources, gathering and maintaining the data needed, and completing and reviewing the collection of information. Send comments regarding this burden estimate or any other aspect of this collection of information, including suggestions for reducing this burden, to Washington headquarters Services, Directorate for Information Operations and Reports, 1215 Jefferson Davis Highway, Suite 1204, Arlington, VA 22202-4302, and to the Office of Management and Budget, Paperwork Reduction Project (0704-0188) Washington DC 20503.			
1. AGENCY USE ONLY ***(Leave blank)***	**2. REPORT DATE** March 2017	**3. REPORT TYPE AND DATES COVERED** Master's thesis	
4. TITLE AND SUBTITLE COMPARISON OF POLARIRIMETRIC CAMERAS			**5. FUNDING NUMBERS**
6. AUTHOR(S) Jarrad A. Smoke			
7. PERFORMING ORGANIZATION NAME(S) AND ADDRESS(ES) Naval Postgraduate School Monterey, CA 93943-5000			**8. PERFORMING ORGANIZATION REPORT NUMBER**
9. SPONSORING /MONITORING AGENCY NAME(S) AND ADDRESS(ES) N/A			**10. SPONSORING / MONITORING AGENCY REPORT NUMBER**
11. SUPPLEMENTARY NOTES The views expressed in this thesis are those of the author and do not reflect the official policy or position of the Department of Defense or the U.S. Government. IRB number ____N/A____.			
12a. DISTRIBUTION / AVAILABILITY STATEMENT Approved for public release. Distribution is unlimited.			**12b. DISTRIBUTION CODE**

13. ABSTRACT (maximum 200 words)

This thesis is an analysis and comparison of two polarimetric imaging cameras. Previous thesis work utilizing the Salsa Bossa Nova polarimetric camera provided null results in the application of the camera in determining operational uses of polarization in the field of remote sensing. The goal of this thesis is to analyze the capabilities of a newly obtained polarimetric camera from Fluxdata and compare the results with the Salsa camera. The Fluxdata camera will also determine if similar polarization signatures are captured between the two cameras. The assumption is that the new Fluxdata camera will be able to capture better quality polarization data that can be used in classifying objects.

14. SUBJECT TERMS Polarimetric imaging, polarimetric camera, remote sensing.			**15. NUMBER OF PAGES** 100
			16. PRICE CODE
17. SECURITY CLASSIFICATION OF REPORT Unclassified	**18. SECURITY CLASSIFICATION OF THIS PAGE** Unclassified	**19. SECURITY CLASSIFICATION OF ABSTRACT** Unclassified	**20. LIMITATION OF ABSTRACT** UU

NSN 7540-01-280-5500 Standard Form 298 (Rev. 2-89)
Prescribed by ANSI Std. 239-18

THIS PAGE INTENTIONALLY LEFT BLANK

Approved for public release. Distribution is unlimited.

COMPARISON OF POLARIRIMETRIC CAMERAS

Jarrad A. Smoke
Lieutenant, United States Navy
B.S., United States Naval Academy, 2010

Submitted in partial fulfillment of the
requirements for the degree of

MASTER OF SCIENCE IN SPACE SYSTEMS OPERATIONS

from the

NAVAL POSTGRADUATE SCHOOL
March 2017

Approved by: R. C. Olsen
Thesis Advisor

D. Trask
Co-Advisor

J. H. Newman
Chair, Space Systems Academic Group

THIS PAGE INTENTIONALLY LEFT BLANK

ABSTRACT

This thesis is an analysis and comparison of two polarimetric imaging cameras. Previous thesis work utilizing the Salsa Bossa Nova polarimetric camera provided null results in the application of the camera in determining operational uses of polarization in the field of remote sensing. The goal of this thesis is to compare polarimetric data between two cameras and analyze the capabilities of a newly obtained polarimetric camera from Fluxdata. The Fluxdata and Salsa cameras utilize two different techniques to capture polarized light. The Salsa uses a Division of Time Polarimeter (DoTP), which is sensitive to movement, and the Fluxdata camera uses a Division of Amplitude Polarimeter (DoAmP), which is designed to split the incoming light without errors from scene movement. The assumption is that the new Fluxdata camera will be able to capture higher quality polarization data that can be used in classifying objects in moving scenes. The results of the study confirmed both camera's display correct polarization signatures and the movement of objects is not affected by the Fluxdata. The Fluxdata displays more detailed polarization signatures, but still suffers from registration errors which are inherent of the focal plane alignment of the DoAmP design.

THIS PAGE INTENTIONALLY LEFT BLANK

TABLE OF CONTENTS

THIS PAGE INTENTIONALLY LEFT BLANK

LIST OF FIGURES

Do not manually type your List of Figures; update this list in the same manner described in Chapter I, Section D.

THIS PAGE INTENTIONALLY LEFT BLANK

LIST OF TABLES

Do not manually type your List of Tables; update this list in the same manner described in Chapter I, Section D.

No table of figures entries found.

THIS PAGE INTENTIONALLY LEFT BLANK

LIST OF ACRONYMS AND ABBREVIATIONS

Required if thesis contains six or more acronyms. The preferred format is to capitalize proper nouns but lowercase common nouns. For capitalization guidance on many acronyms used in the Department of Defense, refer to the *Department of Defense Dictionary of Military and Associated Terms*. Compile the list in alphabetical order, with numbered terms preceding lettered terms, as shown.

2LM	Role 2 light maneuver
APOE	aerial port of embarkation
BHR	Bureau of Humanitarian Response
JLOC	joint logistics operations center
MILOB	military observer
NATO	North Atlantic Treaty Organization
RFID	radio frequency identification
SOFAR	sound fixing and ranging
TLAM	Tomahawk land attack missile
TGIF	thank goodness it's Friday
VA	Veterans Administration
WORM	write once read many
ZULU	time zone indicator for Universal Time

THIS PAGE INTENTIONALLY LEFT BLANK

ACKNOWLEDGMENTS

THIS PAGE INTENTIONALLY LEFT BLANK

I. INTRODUCTION

Polarization is one of the four characteristics of light viewed in remote sensing. Polarimetric imaging is a relatively new field in the remote sensing community. The advantages of polarimetric imaging to detect and categorize objects is not a high priority topic in the realm of remote sensing. The use of polarization in remote sensing and its interaction with the world is yet to be clearly portrayed as a major advantage over traditional panchromatic and multispectral imaging. This research compares and verifies polarization signatures from previous work with a polarization camera. The image comparison confirms the effects of polarization in remote sensing and potential uses.

The primary objective is to determine the similarities and differences of the images captured and compare how each camera captures and depicts the effects of polarization. Additionally, the advantages and disadvantages of the specific techniques and capabilities of the camera's will be analyzed to further understandings of how imaging can be utilized to find a common ground for polarization imaging. The use of these polarization cameras help the human eye distinguish features of both natural and man-made objects that are normally ignored in traditional remote sensing techniques. A brief overview and history of polarization are presented to better understand the analysis of the images collected using the two polarization cameras.

A. POLARIZATION EXPLAINED

Humans view the intensity of light as the various colors of the spectrum. Characteristics of light include amplitude (intensity), frequency (color), polarization, and coherence (Schott, p.4). The human eye has cone cells, displayed in Figure 1, that correspond reflected light from objects into colors which range from wavelengths of approximately 400-700nm (Olsen, p.61). The human eye cannot interpret polarized light, but some insects can view polarized and ultraviolet light. Insects have special photoreceptors that distinguish the electric field orientation which characterizes the polarization effect used by bees and ants to navigate.

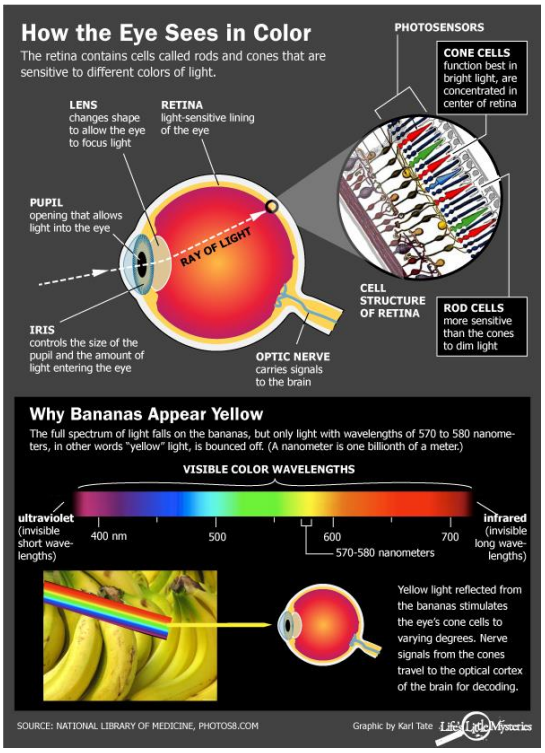

Figure 1. Human eye viewing light. (From Pappas)

The naked eye cannot distinguish polarized from nonpolarized light. Polarized light occurs when a light waves' electric field is on distinct plane perpendicular to the transverse waves. Naturally occurring light can be unpolarized, partially polarized, or fully polarized. Sources of light include the sun, lightbulbs, candles, or any light creating object. Once light encounters a surface, it becomes partially polarized, fully polarized, or remains unpolarized, depending on the surface and angle. The production of polarized light is caused by absorption, refraction, reflection, diffraction, and birefringence. To understand polarization, a basic understanding of the characteristics of electromagnetic radiation through Maxwell's equation is described.

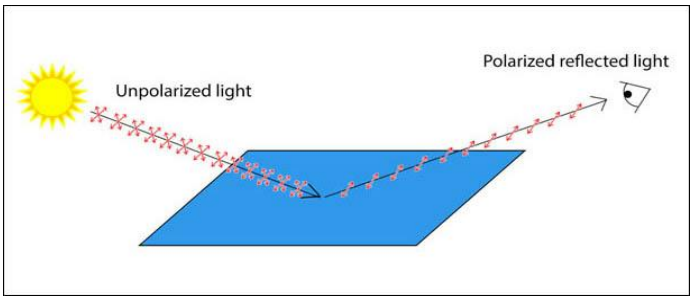

Figure 2. Viewing Polarization after being reflected from horizontal surface. (From Collett)

Maxwell's equations explain electromagnetic radiation and describe polarization for a transverse wave; displayed mathematically and represented in three-axis graph in Figure 3. The direction of the electric field is how polarization is determined. If the electric field is well defined in a certain direction, then the light is polarized. The light is unpolarized if the electric field is randomly oriented without a distinct direction.

$$\nabla \times \mathbf{H} = \mathbf{J} + \frac{\partial \mathbf{D}}{\partial t}$$

$$\nabla \times \mathbf{E} = -\frac{\partial \mathbf{B}}{\partial t}$$

$$\nabla \cdot \mathbf{D} = \rho$$

$$\nabla \cdot \mathbf{B} = 0$$

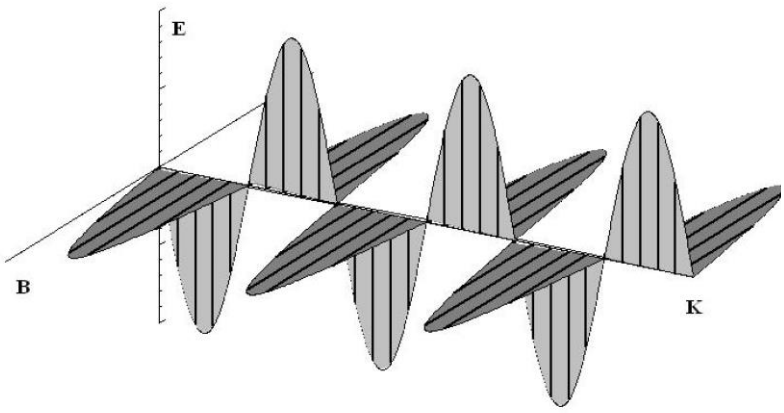

Figure 3. E is the electric field, B is the magnetic induction field, D is the electric displacement, H is the magnetic field, J is electric current, t is time. (From Olsen, p. 30)

1. Viewing Polarization

The simplest way to view a plane of polarization is by removing all unwanted polarization orientations. Viewing an image that allows only vertical polarization will eliminate the light in the horizontal field and all other angles of polarization besides the vertical state. This examples may help improve the appearance of vegetation, eliminate glare from roads, view into bodies of water, or determine objects with polarized material.

The primary and most common way to measure and view polarization is through Stokes parameters. Stokes vector representation of a polarized beam represent both fully and partially polarized beams (Schott, p. 33). An advantage of Stokes vectors is that there is no preferred orientation when associating them with the electric field (Schott, p. 33). Stokes parameters are observable quantities displayed in terms of optical intensities as shown in Figure 4 (Schott, p. 34). The terms S0, S1, S2, and S3 are synonymously referred to as I, Q, U, and V, respectively. The S0 term is the total energy of a beam or intensity of light captured, effectively the unpolarized light (Olsen, p. 140). The S0 term is also how a typical panchromatic image would be represented. S1 is the amount of linear or vertical polarization, also described as the difference between light polarized at 0 and 90 degrees. S2 is the difference between polarized light at +45 and -45 degrees. S3 describes the difference of right and left hand circular polarization. Circular polarization in the S3 term is generally ignored in viewing polarization because it is rarely found in nature (Olsen, p. 140).

$$S_0 = I_{0°} + I_{90°}$$

$$S_1 = I_{0°} - I_{90°}$$

$$S_2 = I_{45°} - I_{-45°}$$

$$S_3 = I_{rh} - I_{lh}$$

Polarization State	Symbol	Stokes Vector
Horizontal	↔ ⊥ S	$\begin{pmatrix}1\\1\\0\\0\end{pmatrix}$
Linear +45 deg	⤢	$\begin{pmatrix}1\\0\\1\\0\end{pmatrix}$
Right-Hand Circular	↻	$\begin{pmatrix}1\\0\\0\\1\end{pmatrix}$
Random	*	$\begin{pmatrix}1\\0\\0\\0\end{pmatrix}$

Polarization State	Symbol	Stokes Vector
Vertical	↕ || P	$\begin{pmatrix}1\\-1\\0\\0\end{pmatrix}$
Linear −45 deg	⤡	$\begin{pmatrix}1\\0\\-1\\0\end{pmatrix}$
Left-Hand Circular	↺	$\begin{pmatrix}1\\0\\0\\-1\end{pmatrix}$

Figure 4. Stokes Vectors. (From Schott)

a. Products of Stokes

Various products can be calculated from the acquired Stokes vectors to display polarization images and video. Some of these calculations include degree of polarization, angle of polarization, inverse intensity, and color mapping techniques. Each of these calculations mathematically calculate each pixel to determine the output product.

The degree of linear polarization (DoLP) or degree of polarization (DoP) is the percentage of linear polarization in the electromagnetic wave. We calculate DoLP using Stokes vectors as seen in Figure 5. Each pixel value is calculated and varies from 0 (unpolarized) to 1 (polarized), with values in between being partially polarized (Presnar).

$$\mathrm{DoP} = \frac{\sqrt{S_1^{\,2} + S_2^{\,2}}}{\mathrm{S}_0}$$

Figure 5. Degree of Linear Polarization(DoLP) or Degree of Polarization (DoP) equations (From Schott, p. 42)

The resulting image represents the fraction of polarization for each pixel. The representation helps distinguish polarized objects. The DoLP is represented with black as 0% linear polarization and white as 100% linear polarizaiton, with values in between as a grayscale.

The inverse intensity is a simple calculation to invert the total intensity of the image and display the objects with smaller intensities in a different manner.

Color combination of Stokes vectors are used to associate Stokes parameters to a color such as Red for S0, Green for S1, and Blue for S2 to distinguish objects with stronger polarizations in each field. Another examples is how J. Scott Tyo displayed an HSV (Hue, Saturation, Value) representation in which the hue is the angle in color space (ranging from 0-360), saturation (ranging from 0 (neutral gray) to 1 (pure color), and value is the brightness of the scene, spanning from 0 to maximum brightness as displayed in Figure 6 (Schott, p.154).

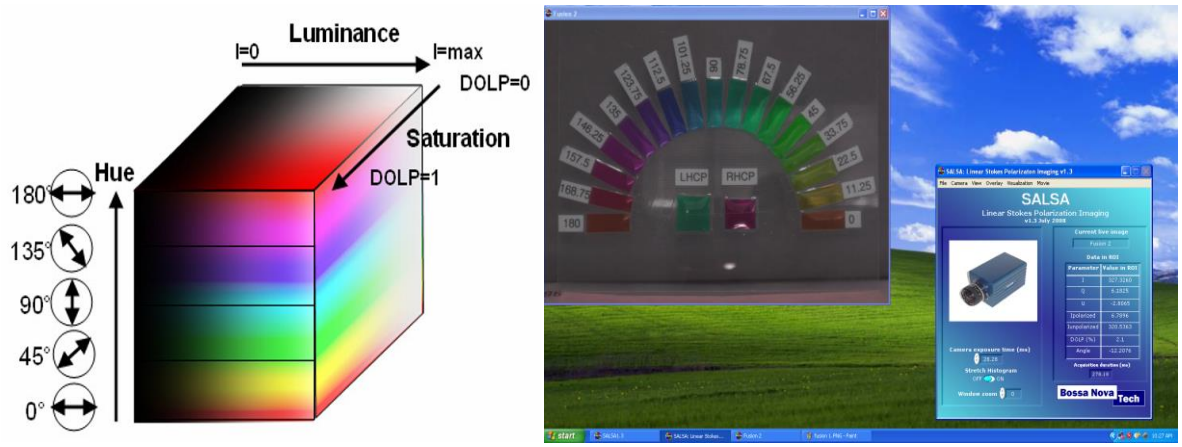

Figure 6. HSV Representation and Salsa Camera example. (From Salsa)

B. OPTICAL POLARIZATION

Optical polarization involves the use of filters to capture light and view scenes in a different perspective. Filters, also known as polarizers, differentially transmit or reflect electromagnetic radiation based on the orientation of the electric field to distinguish polarization. The perfect filter absorbs all of a distinct state of polarization and transmits all other orientations of polarization as show in Figure 7. Polarimetric imaging is used in remote sensing, microscopy, stress testing, and various other sensing fields to discover new characteristics that are not seen through traditional viewing techniques.

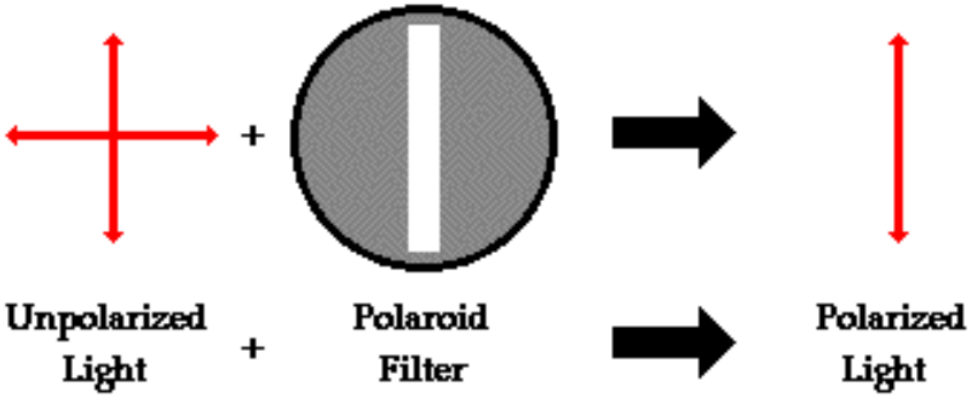

Figure 7. Polarized Filter. From Henderson.

Filters include linear and circular types made of wire grid polarizers, dichroic and birefringent polarizers. Wire grid polarizers and sheet polarizers consist of very thin layers of metallic materials aligned with each other to transmit a specific direction of the electric field, while absorbing or reflecting the perpendicular field, as shown in Figure 8. Similar effects are found in nature in crystals. A dichroic polarizer absorbs a certain polarization of light and transmit the rest, while a birefringent polarizer is dependent on the refractive angle that it absorbs. Including these materials on cameras and detectors aid in the measurement of the polarization state of a beam.

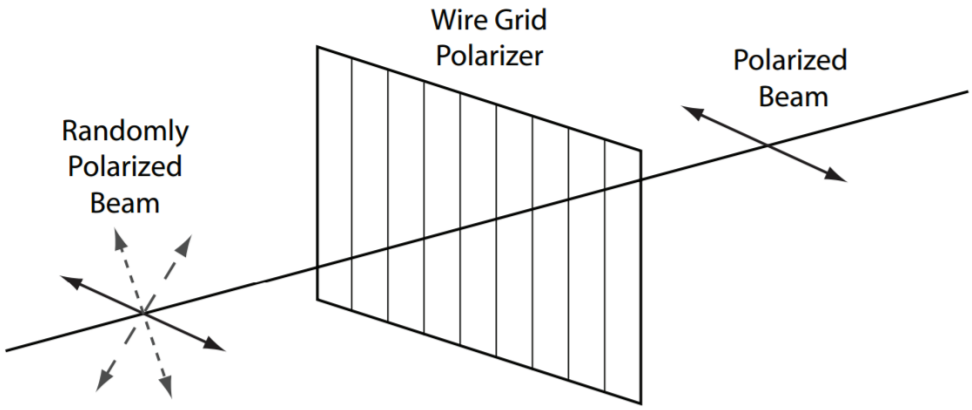

Figure 8. Wire grid polarizer. (From Schott p.55)

Polarimetric interactions in remote sensing describe the behaviors of the polarized beam with a reflective or transmissive medium (Schott, p. 51). Light interacts with surfaces through transmission, reflection, scattering, or absorption as shown in Figure 9. These interactions are based on the physical properties of the object, the wavelength of the incident radiation, and the angle at which the wave hits the surface (Olsen, p. 45).

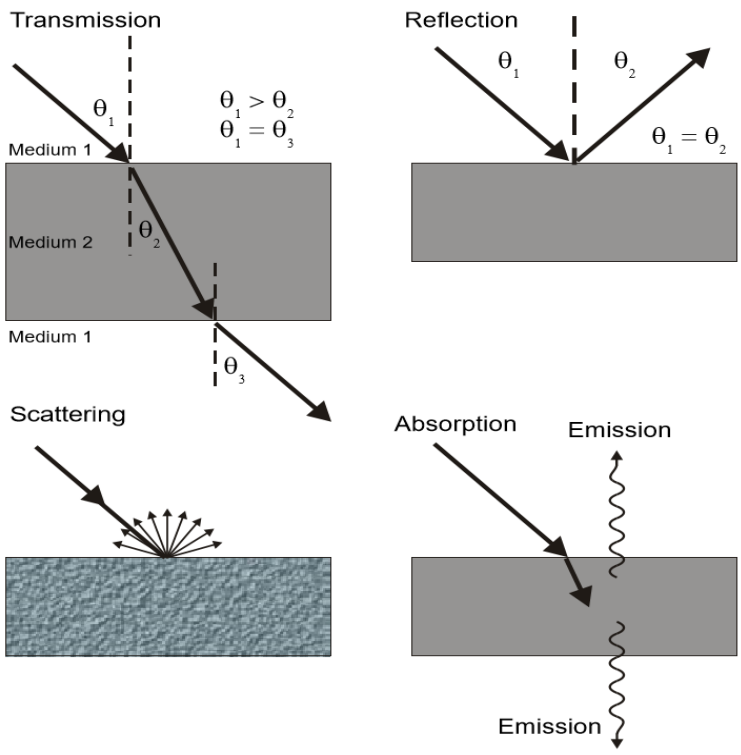

Figure 9. Light interactions. (From Olsen p. 45)

Polarization by reflection occurs when unpolarized light interacts with a surface and the reflected light undergoes a polarization change. Fresnel's equation and depictions in Figure 10 explains how the polarization state change is affected by the angle of incidence, where r is the ratio of the amplitude of the reflected electric field to the incident field and n1, θ1 and n2, θ2 are the refractive indices and angles of incidence and refraction (Olsen, p. 46). Similarly, the transmittance of polarized waves interacts when they pass through matter without a measurable change in attenuation (Olsen, p. 45).

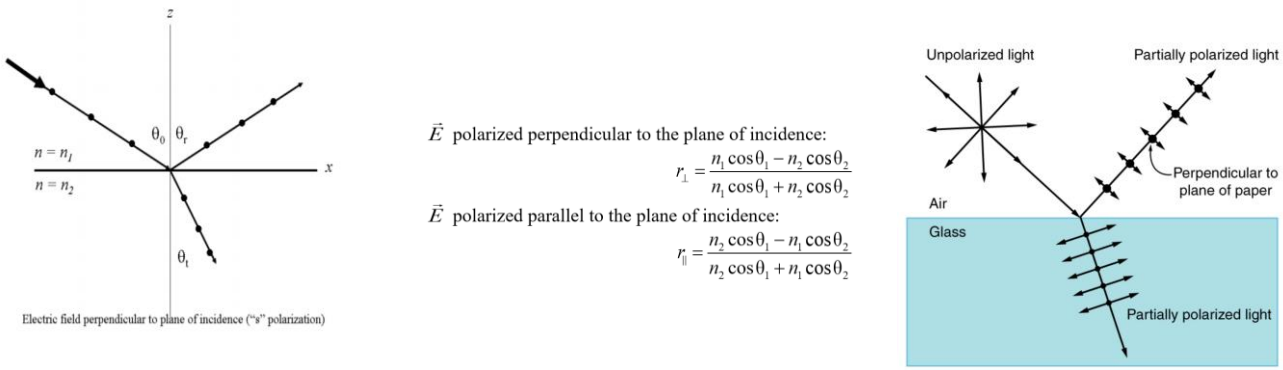

Figure 10. Transmittance and reflectance for polarized light (From Roger Easton)

Polarization by scattering is like reflection but the resulting polarization is dispersed in an unpredictable direction. Rayleigh scattering, depicted in Figure 11, occurs when particles are much smaller than the incident wavelength.

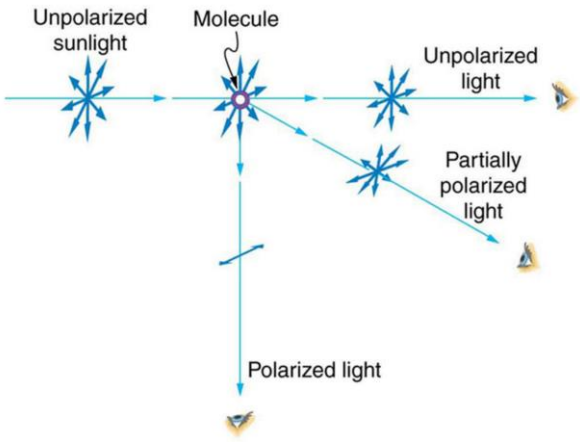

Figure 11. Polarization by scattering. (From Boundless)

Polarization absorption occurs when the incoming radiation is taken in by a medium and not transmitted (Olsen, p.47). Certain crystals and polaroid film uses the process of absorption of polarized states to absorb distinct polarization states.

1. UMOV Effect

The UMOV effect is the phenomenon in which the degree of linear polarization is inversely proportional to a material's reflectance or albedo (Schott, p73). Interparticles scattering causes an increased albedo and decreased polarization (Zubko). An object with a bright surface will tend to have a lower degree of polarization and darker objects will have higher degrees of polarization. Quantitative data has been collected on the moon that displays the UMOV effect for different phases and regions of the moon (Zubko). The effect relates the wavelength, color, and texture of an object to polarization.

C. NON-OPTICAL POLARIZATION

Communications and radar applications also utilize polarization to control electromagnetic radiation to propagate signals. Both linear and circular polarization waves are used to transfer information and receive electromagnetic radiation. Polarized filters work similarly in the non-optical field with the type of antenna chosen when sending and receiving data. Antennae have the capability to transmit and receive various horizontal, vertical, and circular radiation formats. One example is a right hand circular antenna may only accept other right hand circular signals, thus eliminating other signals being transmitted. Radar antennae work in a similar fashion to transmit signals and receive the requested polarization signal to determine objects and images. A design of dual polarization radar sends both vertical and horizontal electromagnetic waves and computes cross sectional areas to classify size and shapes of objects with improvements in rainfall estimation, precipitation classification, data quality and weather hazard detection (NOAA).

D. MODERN APPLICATIONS OF POLARIZATION

The most common use of polarization in everyday use are polarized sunglasses. This technology eliminates glare from vectors of polarization that are reflected from roads or water. Most glare comes from horizontal surfaces such as highways and water. A pair of sunglasses designed to eliminate glare might be vertically polarized to eliminate the horizontal glare and only allow vertically polarized light through the glasses.

Some light sources are polarized such as lasers and monitors. Certain television or computer monitors have polarized films or layers to control the intensity of light viewed by the user. Liquid Crystal Displays (LCD) use polarization to control different intensities of colors. Not all lasers are polarized, but some devices such as interferometers, semiconductor optical amplifiers, and optical modulators use polarized lasers to achieve their desired results.

Displaying 3D movies and images is possible because of polarization. 3D imaging uses two images overlaid on the same screen with the use special polarized glasses creating a 3D image. With a different polarized filter on each lens, the human eye sees two images that create the 3D image.

The use of polarization in microscopic science has led to the discovery of how different anisotropic substances interact with polarized light. Anisotropic substances interact differently under polarized light and do not behave the same way in all directions. Polarization microscopes are used in medical fields and geological research. The basic concept and design of a polarizing microscope is displayed in Figure 12.

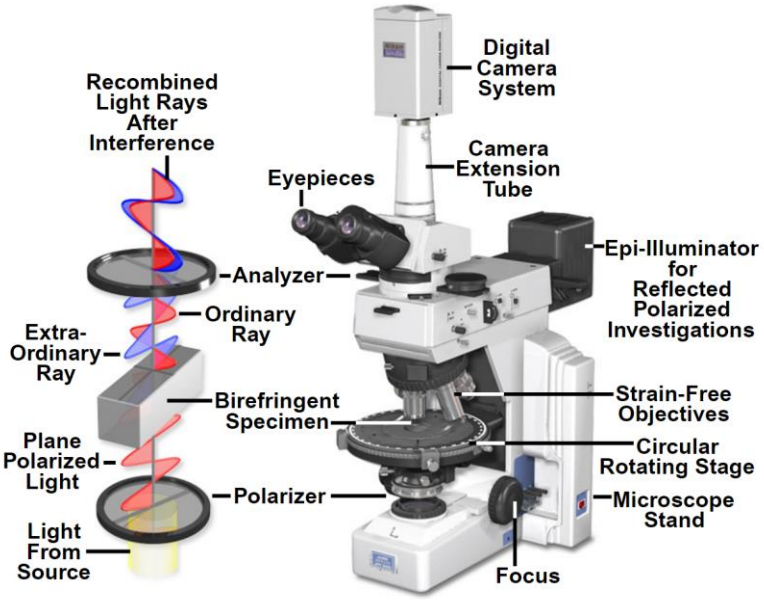

Figure 12. Polarizing Microscope. (From Robinson)

Satellites and radar utilize polarization in the optical and non-optical fields. Communication and radar imagery use polarization to transfer information in military and commercial products. Synthetic Aperture Radar (SAR) onboard TerraSAR-X and airborne assets such as AIRSAR utilize different polarization signatures when imaging (Lou). Figure 13 displays a product of polarized radar imagery.

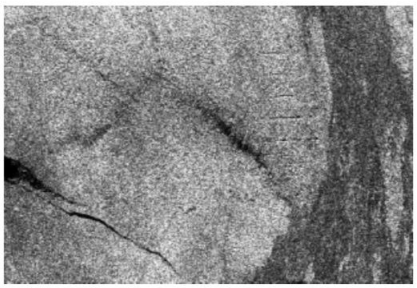

C-Band HH

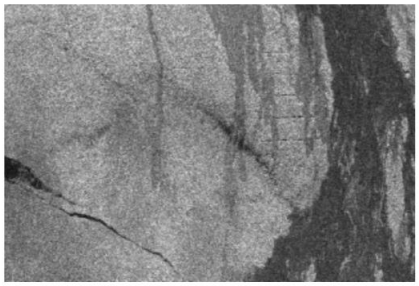

C-Band HV

Figure 13. Polarized RADAR imagery. (From Smith, Randal)

II. HISTORY

The origins of polarization date back to the eleventh century with experiments verifying the ray theory of light and the law of reflection (Collett, p. 1). Polarization observations began in scientific studies in the late 19th century with early understandings dating back to 1669 (Brosseau, p. 1). Through folklore, the possibility of Vikings using polarization of the sky light to navigate dates to 700 (Brosseau, p.3). The history of polarization studies can be broken down into three distinct research periods that lead us to the modern study of polarization based on ideas and observations from Bartholinus to Stokes, the electromagnetic nature of light, and the coherence and quantum properties of light.

A. FIRST PERIOD: 1669-1864

In the seventeenth century, the study of polarization started with the optical observations of light and geometric measurements showing that it as an instantaneous propagation of an action through a medium (Brosseau, p. 3). Erasmus Bartholinus is typically given credit in discovering polarization in 1669 with the demonstration of double refraction using a crystal made of calcite (Brosseau, p. 3). Depicted in Figure 14, Bartholinus showed how a single ray of light consisted of two separate rays when propagated through a rhombohedral calcite crystal. Shortly after, Dutch physicist, Christiaan Huyghens, added a second calcite crystal and determined that the two beams passing through a second crystal could be manipulated to maximize and minimize the intensity of light, demonstrating different polarization directions (Brosseau, p. 4). Huyghens developed the geometric theory to determine all optical occurrences including reflection, refraction, and double refraction (Brosseau, p. 4). Following these discoveries, Newton's particle theory of light verified light as a beam comprised of rays identified by geometric lines consisting of streams of particles (Brosseau, p. 4). Following these discoveries, Newton's great standing and views on light led to a slow development of polarization until the establishment of the wave theory of light in the nineteenth century.

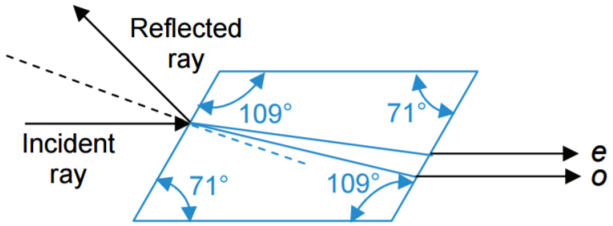

Figure 14. Double refraction (From Collett)

In 1803, Thomas Young displayed the effect of polarization from the transverse nature of light, which countered Newton's concepts on destructive interference of light (Brosseau, p. 4). Etienne-Louis Malus discovered the polarization of natural light by reflection. He experimented and geometrically reasoned how to explain the intensities of light from a polarizing crystal. His worked shows how to filter out polarized light and Figure 15 displays the effects of a how natural incident light becomes polarized when reflected by glass. He showed how the light reflected could be extinguished at an approximate angle of incidence of 57-degrees.

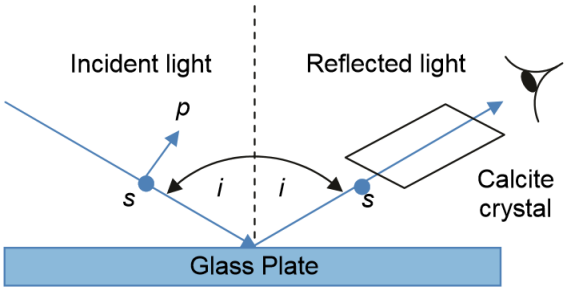

Figure 15. Malus's Glass Plate (From Collett)

Expanding on Malus's glass plate experiment, Sir David Brewster discovered the relation between the refracted ray and incidence angle when observing light through a crystal reflected off a glass surface (Figure 3.). He determined that there is a particular

angle of incidence that extinguishes light and that complete polarization occurs when the angle of incidence equals this angle (Brewster's angle) (Brosseau, p. 5). The Brewster angle determined the neutral point of polarization in the sky.

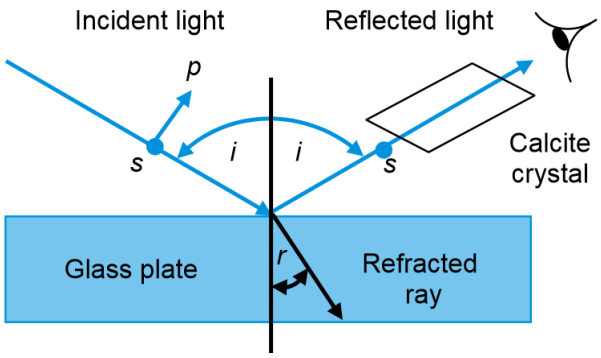

$$\tan i = n_2 / n_1 = n. \quad i + r = 90°.$$

Figure 16. Brewster's Law (Collett)

Augustin Jean Fresnel furthered the understanding of the modern view of polarized light and the wave theory of light with his work on reflection and transmission formulas which recognized the phenomenon of certain material to have an index of refraction for right and left circular polarized light (Brosseau, p. 5). Along with Faancois Arago, Fresnel contributed to the laws of interference of polarized light. These laws describe the effects of linearly polarized and linearly polarized with orthogonal polarizations and how they interfere when interacting. Additionally, the creation of the optical microscope and polariscope in the nineteenth century advanced studies in the polarization signature details of minerals and various materials (Brosseau, p. 6).

Sir Georges Stokes introduced the Stokes parameters, which were measurable quantities of the properties of polarized light. The Stokes' parameters mathematically describe the state of polarization, to include partially and polarized light (Brosseau, p. 7). His explanation of the polarized light was based on intensities at optical frequencies, with

the first parameter signifying total intensity and the remaining three describing the state of polarization for linearly, diagonal, and circular polarization.

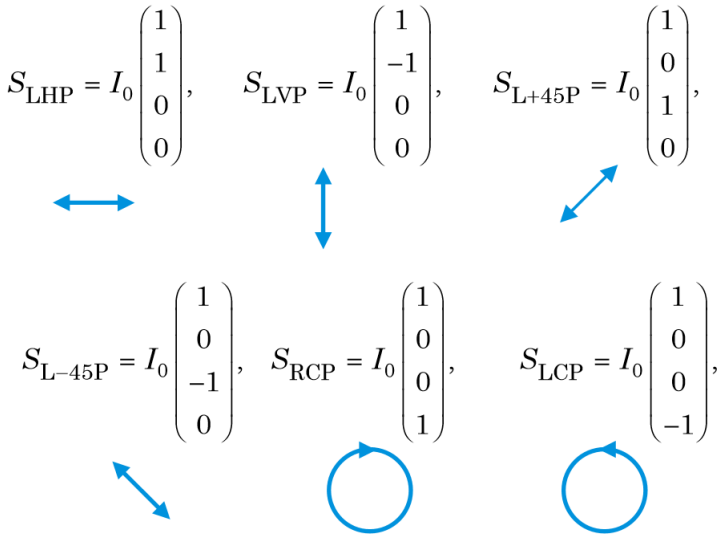

Figure 17. Stokes Vectors. (From Schott)

Giorgo Govi's experimentations on light concluded that small particles scattering light is a marvel that is not reliant on the refection of light, leading to the research of the scattering of radiation by matter. Govi's research helped pave the path for John Tyndall to demonstrate the scattering of light by particles was dependent on particle size and how very fine particles perfectly polarize light at a 90-degree angle (Brosseau, p. 8). Tyndall's research in 1869 led to inventions to conduct research about the color of the sky and water.

B. SECOND PERIOD 1864-1920

Maxwell's theory of the electromagnetic (EM) nature of light established a new era of observation and research in the polarimetry field of science. Maxwell's differential equations based on Faraday's concepts put EM waves into transverse wave solutions. His theory of the EM characteristics of light led to new research of unpolarized and

polarized light with application of polarizers, electric fields, and magnetic fields by scientists including John Kerr, Emile Verdet, and many others (Brosseau, p. 11). An example is Pieter Zeeman's experiments and how he predicted the nature of polarization based on EM fields, further verifying the acceptance of the EM theory of light (Brosseau, p. 12). These discoveries also involved research in other fields including radio and microwave communications.

Lord Rayleigh's contribution to polarization includes his theory of polarization at 90-degree angles and the intensity of light scattered by particles. Rayleigh's law of polarization at 90-degree describes scattered light's highly linearly polarized properties in the sky. His law on intensity of light explained the correlation of the dependence of the degree of polarization from scattered light on the angle of its scattering. Additionally, Nikolay Umov, conveyed the relationships between polarization and surface roughness (Brosseau, p. 13). These theories led to major advancements in understanding the scattering of EM waves by a sphere.

C. THIRD PERIOD: 1920-PRESENT

The final phase of research in polarization's process of emission and absorption by matter was best explained by the end of the nineteenth century with the development of the quantum theory in the twentieth century. Maxwell's theory explained the observable features of light and the quantum theory led to the acceptance of photons. The quantum treatment of polarization was studied and researched to relate back to the classical understanding of polarized light based on the theory of the coherence of light.

The invention of the modern sheet polarizer was developed in 1927 by orientating crystalline needles of herapathite in a sheet of plastic. This invention focused attention on describing changes in the state of polarized light and how it undergoes change while interacting with optical elements. 1928 marked the first use of polarization in remote sensing of planetary surfaces by French astronomer Bernard Lyot (Brosseau, p. 19). Lyot invented optical devices including the double-refraction filter and a depolarizer consisting of two retardation plates, with a retardation ratio of 1:2 and their axes oriented at 45-

degree to another (Brosseau, p. 19). Depolarizers are used to transform polarized light into unpolarized light, which is essential in modern day fiber optics devices.

The term ellipsomtery describes the effect insects utilize to orient themselves with their eyes by using the polarization of sky light (Brosseau, p.19). This led to the discovery of the human eye being able to detect and distinguish the difference of left and right hand circular polarized light, with the understanding that the human eye is not capable of distinguishing linear polarization. Much advancement in communication theory was developed around World War II, including mathematical and statistical properties of polarization that helped develop radar that could detect aircraft.

The brief history of polarization gives a great insight on how the theories and experiments developed into today's modern uses of polarization. Reviewing the progress made through these three major periods, we can implement old and new ideas into the study of polarization for remote sensing today. These concepts will be applied in the analysis of the images captured with polarimetric cameras and help verify polarization states and signatures.

III. CAMERA OPERATIONS

A. SALSA

The Bossa Nova Tech Salsa polarization camera offers both polarization analysis and regular digital video camera capabilities. The easy plug-and-play use of the Salsa makes it easy to setup and take images. The ability to display full Stokes parameters and calculations in real time on each pixel is the main feature in the Salsa camera. The Salsa camera comes with specialized software that provides real time calculations and is easy to use view and output data.

Figure 18. Salsa camera (From Salsa)

The Salsa camera technology uses a patented polarization filter based on an ferroelectric liquid crystal which reduce the acquisition time when taking images. The Salsa's fast switching liquid crystal polarizing filter separates polarized light onto a 782 x 582 pixel detector operating in the 400 to 700 nm range (West). The camera has a standard 12-bit CCD lens, one megapixel, and F mounted lens that is interchangeable. The Salsa has an ARSAT H 20mm with an F number of 2.8 and uses an Hoya 52mm green filter which allows the LCD polarizer to operate within the specified spectral

bandwidth from 520-550 nm. The camera has is powered by a fifteen-volt direct current and has a firewire and USB connection for data input/output to a connected computer. The camera's parts are mounted in a small rectangular box (4"x4"x6"), as depicted in Figure 19.

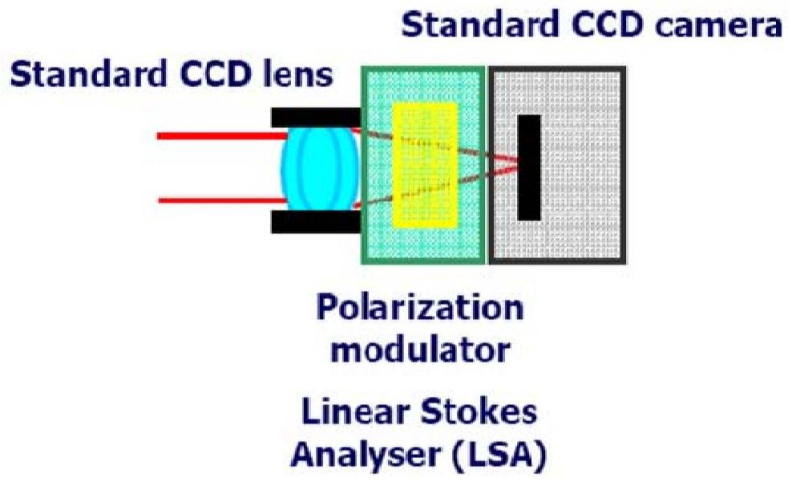

Figure 19. Salsa Camera Mechanism (From Salsa)

The Salsa uses a division of time polarimeter (DoTP) to capture imagery. It uses sequential images taken with the polarization filter rotated to different orientations to construct the linear Stokes vectors. The software then calculates the Stokes vectors pixel by pixel using a modified Pickering method shown in Figure 19. The limitation in the Salsa is that movement in the target or camera results in a miscalculation between each pixel in the rotating frames. This restriction limits the Salsa's use to laboratory and static scenes.

$$S_0 = \frac{\Phi_0 + \Phi_{45} + \Phi_{90} + \Phi_{-45}}{2}$$

$$S_1 = \Phi_0 - \Phi_{90}$$

$$\mathrm{S}_2 = \Phi_{45} - \Phi_{-45}.$$

Figure 20. Modified Pickering Mehtod. (From Schott p139)

The software provided with the Salsa camera was utilized on a Macbook Pro Bootcamp running Windows XP. The Bootcamp image has an Intel Core 2 CPU, 2.33 GHz processor and 2GB of RAM. The Salsa measures intensity and cycles through polarization angles of approximately 0, 45, 90, and 135. These angles correspond to the frames the Salsa calculates the Stokes vectors, but are not exact angle measurement, rather the camera is designed to perform image modulation at orthogonal angles to each other. The camera's software calculates Stokes vectors and various other representations to include DOLP, angle as a color hue, angle, virtual polarization and various other representations of polarization as shown in Figure 20. Each pixel is calculated to provide precise polarization results. There is no registration of images required for the Salsa camera.

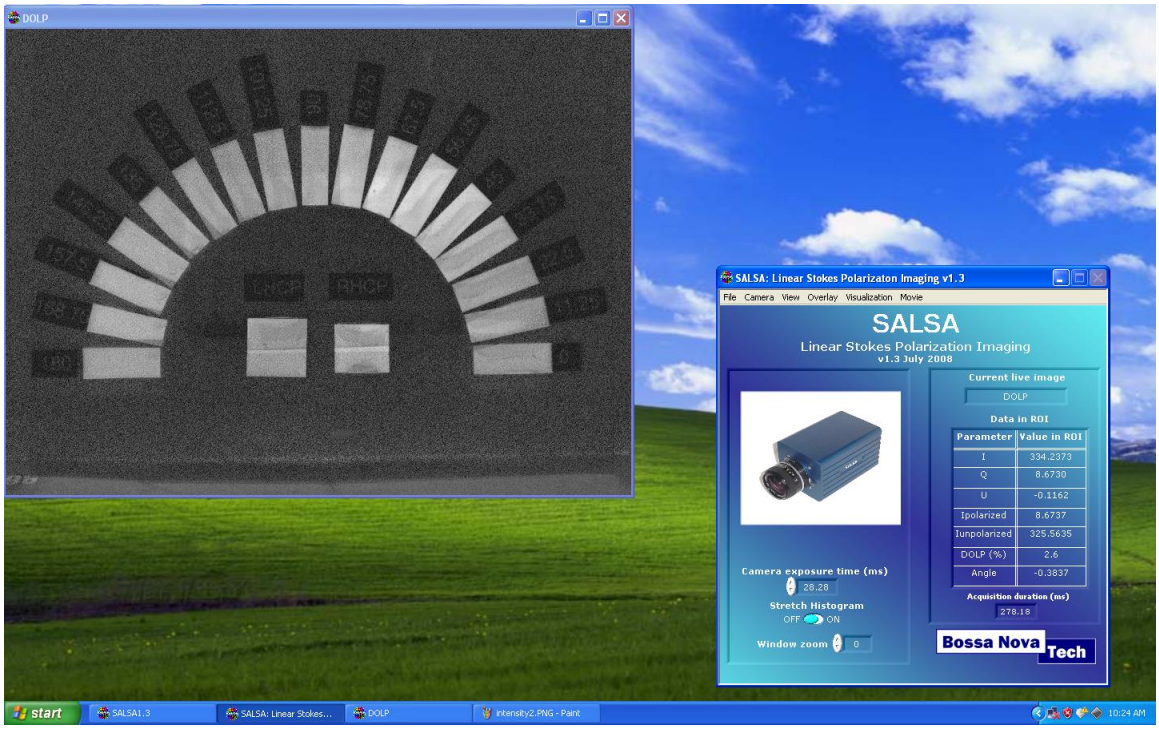

Figure 21. Salsa Software live imagery.

The Salsa software allows for a simple output to save all files or select certain files. The main files utilized to compute products from Stokes vectors are .txt files which contain the pixel by pixel values for I (S0), Q (S1), and U (S2). The .txt files are used in IDL to perform Stokes product representations.

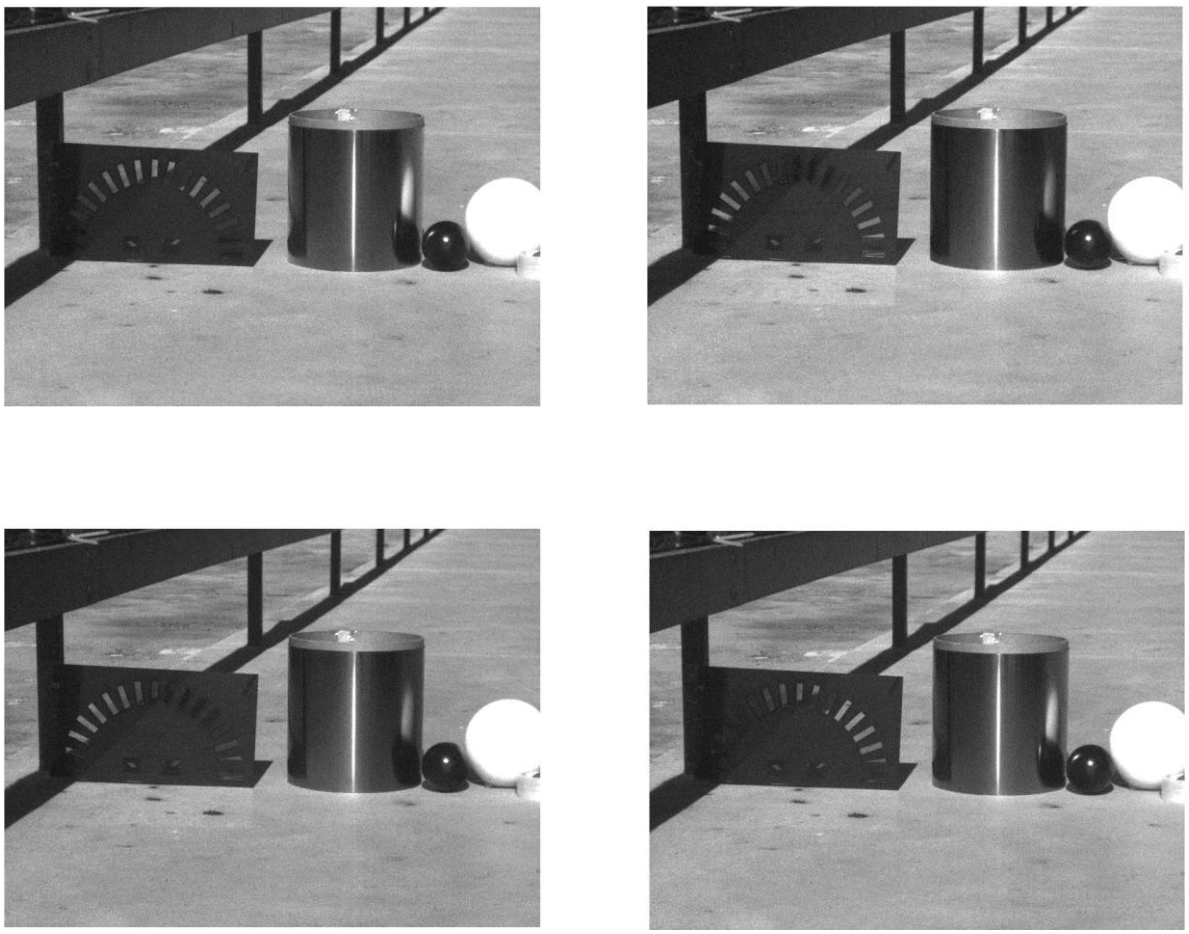

Figure 22. Salsa polarization filter frames. Frame 1(top left) , Frame 2 (top right), Frame 3 (bottom left), Frame 4 (bottom right)

B. FLUXDATA

The Fluxdata FD-1665P 3 CCD Camera is capable of capturing video and images at three linear polarization directions concurrently without time delay in full color. The ability to simultaneously capture imagery without sequential switching of filters eliminates timing and movement issues. This design puts more control in the user's hands and requires the user to interact more with the data to view Stokes parameters and product calculations.

Figure 23. Fluxdata camera

The camera sensor type is a Progressive Scan Charge Coupled Device (CCD) Sony ICX285 with a sensor size of 1628 x1236 pixels. At full resolution, the camera is capable of 30 frames per second. This CCD sensor converts light into electric charges that process to electronic signals for digital images. The CCD relies on the photoelectric effect to establish an electrical signal from the incoming light captured. The camera offers 1.4 megapixels and an F mounted lens that is interchangeable. A NIKON NIKKOR 28mm with an F number of 2.8 was used in the cameras operations. The Fluxdata comes in a compact design measuring (4.6”x3.5”x4.4”).

The Fluxdata features three CCD sensors on three polarizers as depicted in Figure 23. This concept utilizes division of amplitude polarimeters (DoAmP) which avoids timing issues observed using DoTP. The 3-way beam splitting prism is assembled with multiple non-polarizing beam splitter coatings. Two coatings layer the prism to split the incoming light into three components with equal spectral components. Additionally, linear polarization trim filters are positioned in front of each CCD sensor to provide spectral selectivity. DoAmP avoids timing issues by capturing images simultaneously and then splitting the beam into three equal analyzers before being refocused onto their focal planes. This results in three full resolution images that can be used to calculate Stokes vectors pixel by pixel using a modified Pickering method. The issues that arise using DoAmP is aligning the images on the focal plane because of the complex optical paths (Schott, p.147).

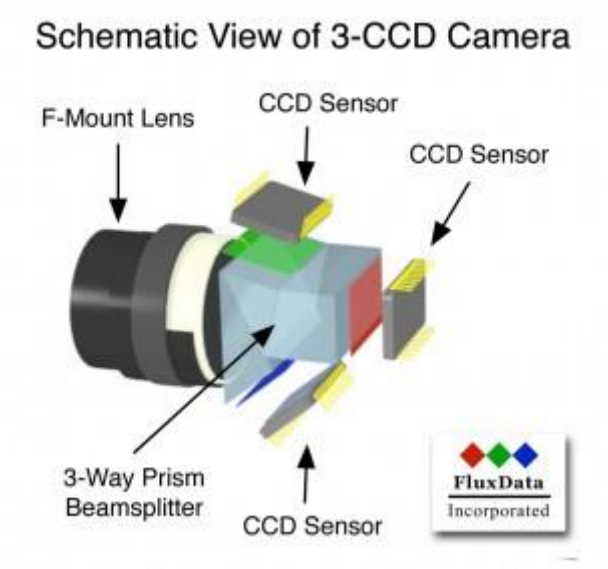

Figure 24. Fluxdata Color CCD sensors (From Fluxdata)

The Fluxdata camera's polarization filters are oriented at 0, 135, and 90 degrees. Traditionally, the Fluxdata camera's polarization filters are oriented at 0, 45, and 90 degrees. The change in the 45 degree filter to 135 was discovered during testing and target detection using a polarization angle filter wheel as depicted in Figure 26. This change in filter alignment causes a more heavily focused 135 angle in the S2 calculation rather than the traditional 45 degree calculation. The S2 calculation appears to be an opposite image as compared to the Salsa's S2. To compensate for the 135 degree filter, S2 was calculated to display positive values in the same way the Salsa camera functions. No major impact was observed during the testing of the camera. The ability to output data prior to Stokes calculations is a feature that is not available on the Salsa.

The Fluxdata utilized a Lenovo X250 laptop running Windows 7 with an Intel Core i5 and 8GB of RAM. The camera is powered by 8V DC ~30V DC, 840mA 12V DC (10W) via a Hirose 12-pin general purpose input-output connector trigger which can be connector to direct power or a battery pack. The camera utilizes 3 GigE (CAT 5) connections with a NETGEAR ethernet switch to connect the channels via CAT 5 to the laptop for high speed data transfer of each channel.

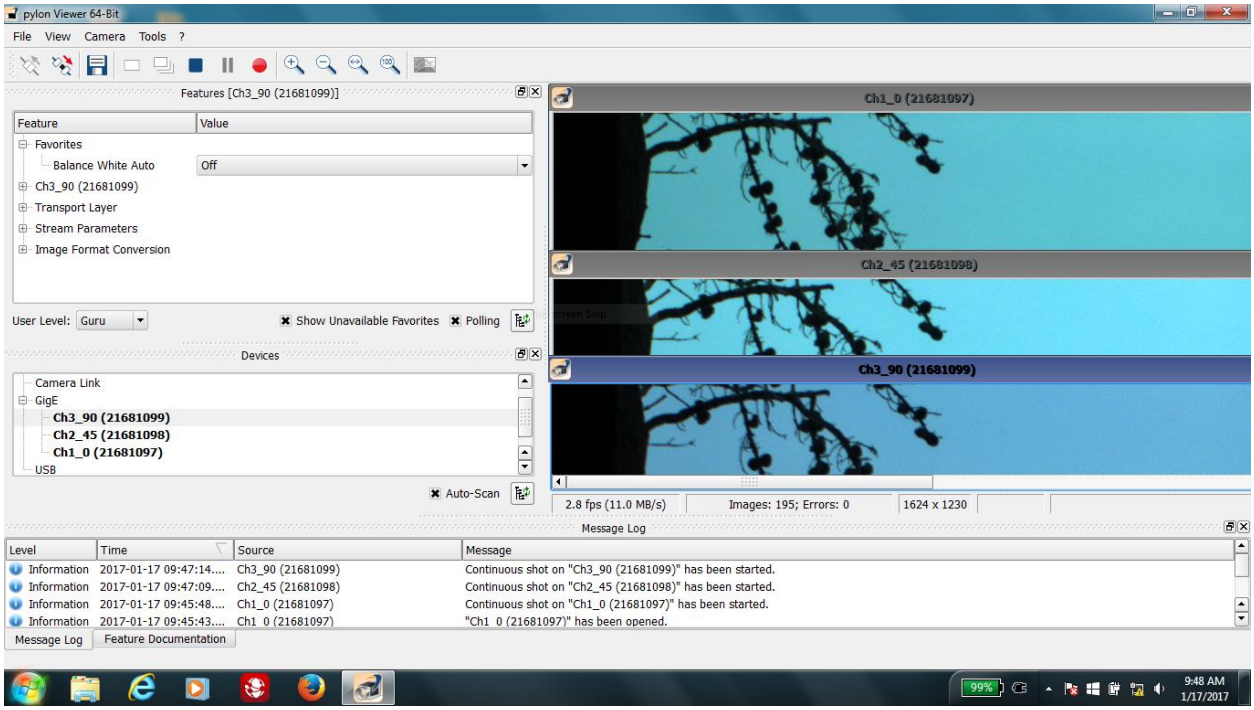

Figure 25. Fluxdata Software Interface

The camera uses the Basler software Development Kit and View Application Field Kit, running Pylon version 4, 64 bit viewer. The software supports various inputs including GigE Vision, IEEE 1394, Camera Link and USB3 Vision Standard. To communicate with the software the computer was set with a static IP on the same subnet as the camera with each channel of the camera set.

The software can be operated in three modes based on the user's level of skill, from beginner, expert, or guru. Each level includes different options to alter to gain the best quality image and use functions such as the trigger mode.

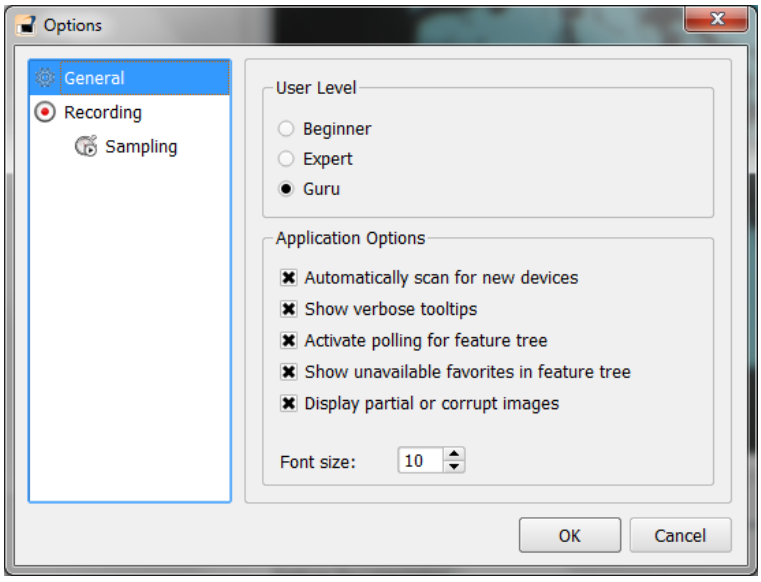

Figure 26. Fluxdata User Settings

The output for the Fluxdata requires the user to trigger embedded software to capture three simultaneous images. To achieve a triggered result a main channel must be selected to act as the primary controller of the other two channels. Selecting the single shot button on the primary channel will trigger the other images to stop. After triggering all input channels to stop the user must individually save each .tiff file for 0, 45, and 90 degrees. The trigger software and settings do not work every time and a closer analysis must be completed by comparing and registering the photos after saving them. If the trigger mode was unsuccessful the images results cause errors in registration. An attempt at creating a standard operating procedure was made but resulted in errors on certain occasions. The exact cause of the trigger mode error was not determined.

The Fluxdata does not perform any computations of Stokes vectors or products. Only the live images and video of 0, 45, and 90 degree polarization filters can be viewed while setting up and preparing a capture. Computation of Stokes must be completed after saving the .tiff files using IDL or Matlab to compute each pixel to Stokes.

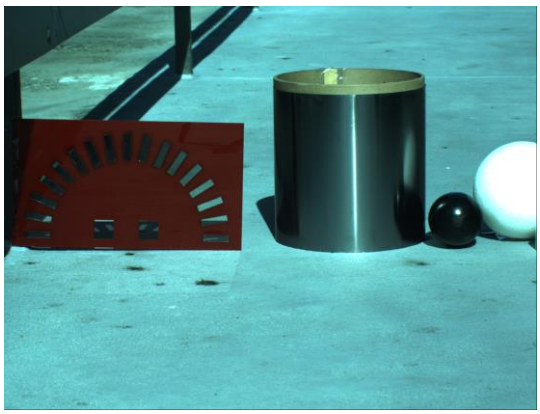 Channel 0, 0 degree	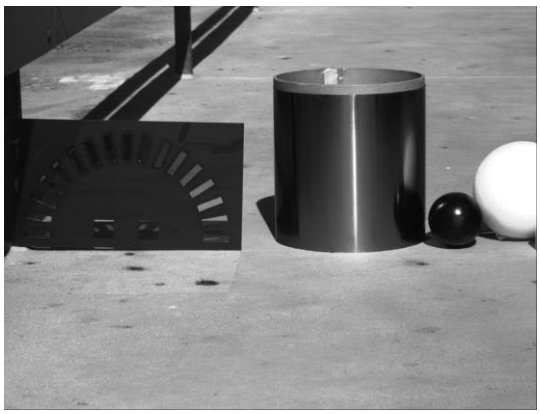 Registered 0 degrees
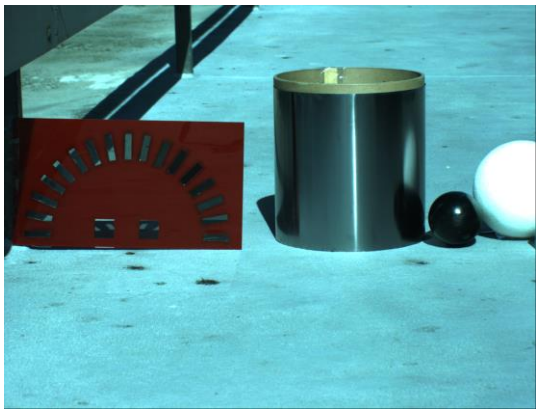 Channel 1, 45 degrees	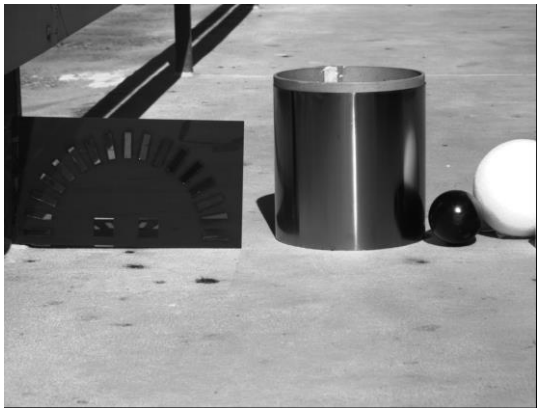 Registered 45 degrees
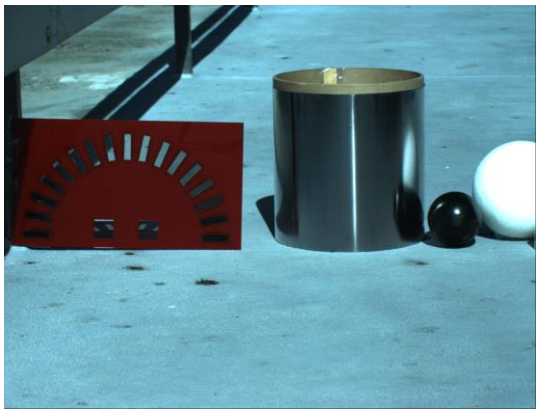 Channel 2, 90 degrees	 Registered 90 degrees

Figure 27. Fluxdata Input/Output Channels (left) and Registered Images (right)

Each channel offers a set of features to control analog and digital controls of the process as displayed in Figure 26. The ability to manipulate each channel gives the user much control to counter the effects of gain and saturation effects.

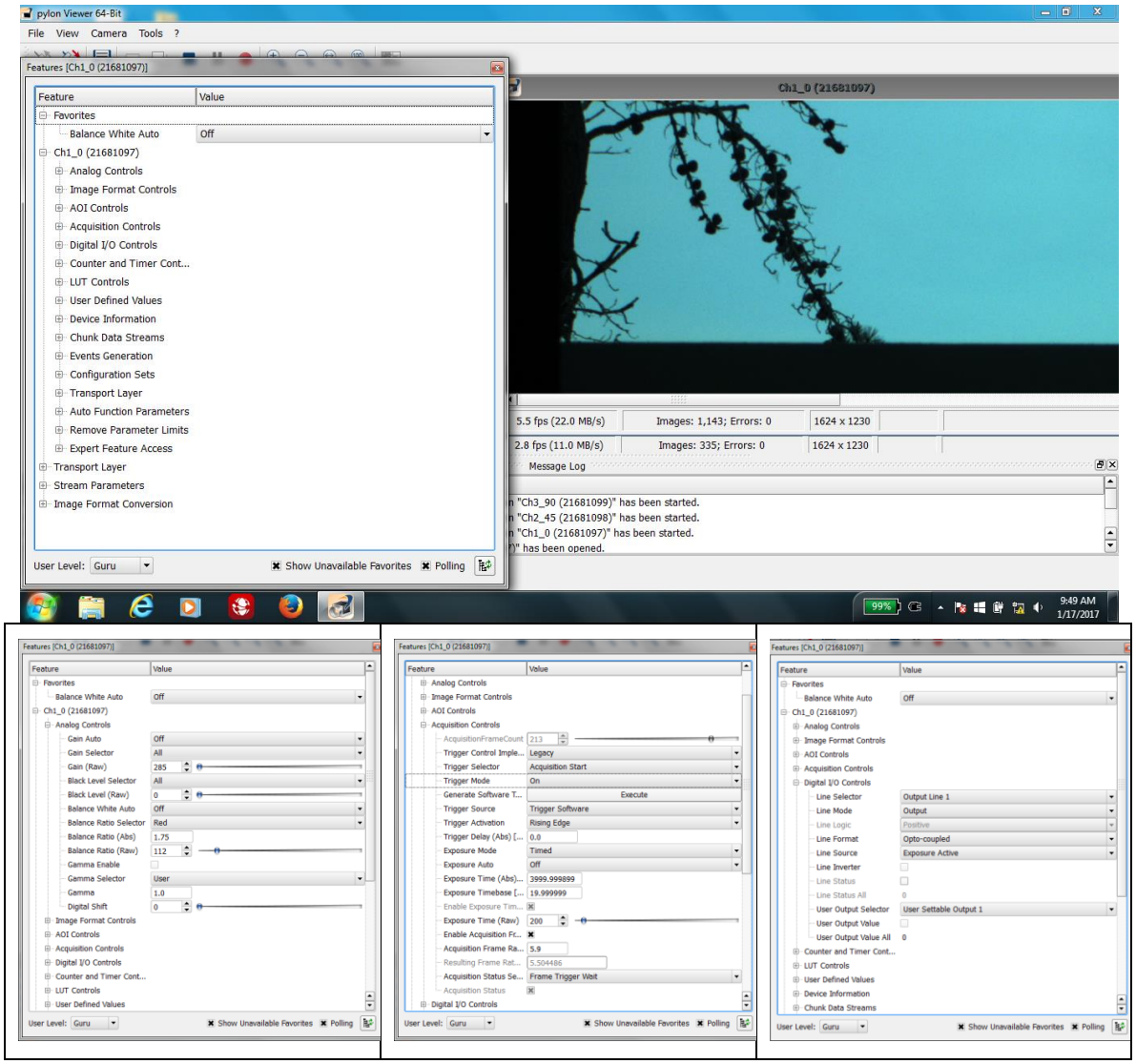

Figure 28. Analog functions, Acquisition controls, and digital I/O controls.

IV. METHODOLOGY

The method of capturing images consisted of both cameras on tripods at similar angles to the scenes being captured. The images were taken at approximately the same time to obtain results from a similar sun angle. Although the results are slightly different when viewing the imagery in respect to size, resolution, and quality, the larger aspect of determining how the cameras determine polarization are compared using ENVI.

Figure 29. Camera setup

The comparison of the cameras and images was based closely to how modern day cameras on phones are tested. Concepts of the ease of use, quality of photos, cost, support, and various details are analyzed to determine the best use of each camera and how a customer would best utilize this emerging technology.

Figure 30. Initial Test

To compare the images, the software program ENVI 5.3 (Environment for Visualizing Images) was used, along with IDL 8.5 (Interactive Data Language) to manipulate the raw data to create and view Stokes vectors and products. ENVI by Harris is software that does image processing and analysis for remote sensing. Functions in ENVI such as band algebra and histogram manipulation were used to compare the Fluxdata and Salsa images. IDL is a programming language that was used to process the .tiff images to create Stokes parameters. Prior to using ENVI or IDL, the Fluxdata images were converted to grayscale and then registered using MATLAB in order to use IDL to convert the polarized images to Stokes measurements.

The total intensity captured by both camera's varied greatly and manipulation of the histogram scale in ENVI was utilized to scale the image and eliminate noise and saturation.

V. DATA ANALYSIS

The data was analyzed both qualitatively and quantitively using ENVI. Various scenes of the Naval Post Graduate School Campus and downtown Monterey, California were captured between July and December of 2016. When viewing the images, a color representation is displayed following columns of images from the Fluxdata and Salsa. After a comparison of the two camera's, the Fluxdata images are displayed with the three Stokes representations and DoLP.

When viewing the grayscale images, the intensity is represented by the brightness of the image. For example, S1 image is brighter in the horizontal 0 degree polarization, and darker in the vertical 90 degree angle, with gray colors not having a strong signature in either direction. Additionally, various issues with gain and over saturation are a problem with both the Salsa and Fluxdata and can be seen in certain objects. IDL was utilized to scale the images and remove the over saturated data.

Viewing the Stokes vectors in grayscale portrays the stronger signatures in either white or black, with gray representing electric fields received without a distinct polarization state. S0 represents the overall intensity in grayscale, basically a camera without polarization filters and does not represent ant differences between polarizations. S1 displays brighter white positive value as horizontally dominating, while black negative value is vertically dominating, with gray values not having a strong signature. Similarly, S2 displays brighter white as +45 dominating and darker black values stronger in 135 degree dominating. Finally, DoLP scales the polarization from bright white as 100% linear polarized to dark black as 0% linear polarized.

The first objective in comparing the cameras was to compare the Stokes images. The resulting calculations from each camera portray similar results. A polarization angle wheel, which consisted of polarized film arranged at angle from 0 to 180 degrees helps verify the angles of polarization being filtered. The images was taken at 1158 PST on 6 October, 2016 Alongside the wheel, is a cardboard circular cutout wrapped in a highly reflective metal sheet, followed by a bowling pin and a white Styrofoam ball. The

Fluxdata displays a higher resolution image with more detail as compared to the Salsa Stokes. An advantage in the Fluxdata is the detail and differences captured in the background. The brighter portions of S1 signify stronger polarization in the horizontal field, while darker portions of the grayscale images indicate vertical polarization. Similarly, brighter portions of the S2 image show +45 polarization while darker show -45(135) polarization. The DoLP is the main product from the Stokes that helps determine how polarized the contents of an image are. Brighter portions confirm a higher percentage of polarization and darker (black) portions show no polarization signature. Using the polarization filter wheel as a starting point confirms the signatures of the Stokes images and gives a reference to refer to when viewing scenes to detect polarized items of interest. The static target confirms that both cameras calculate and portray Stokes vectors correctly and give a reference for future analysis.

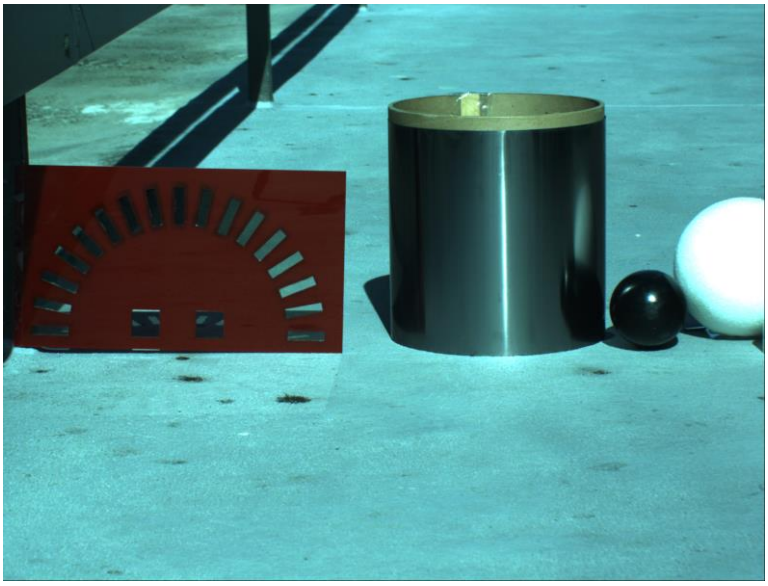

S0

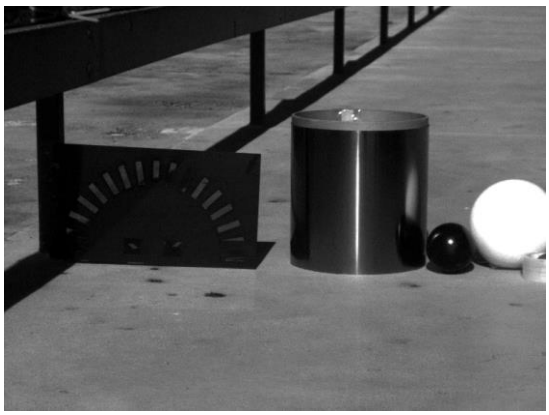

S0

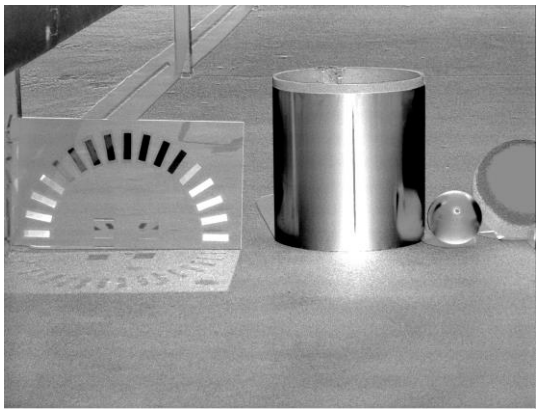

S1

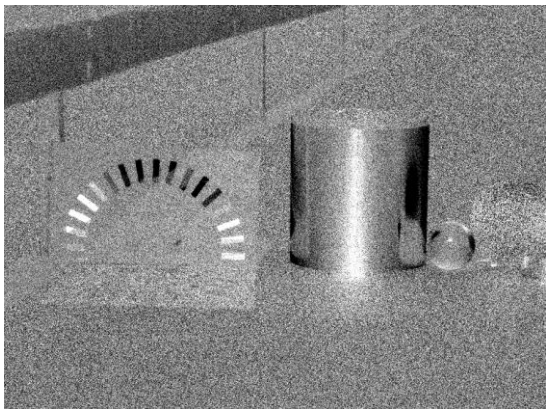

S1

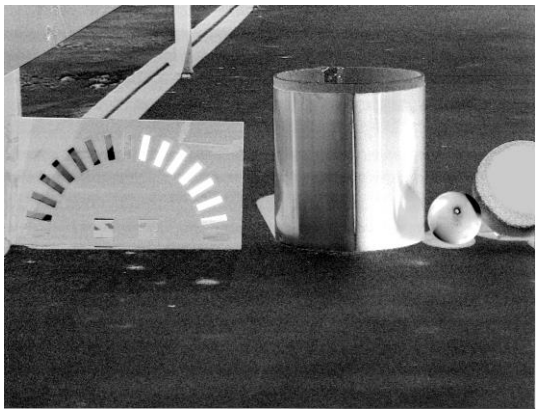

S2

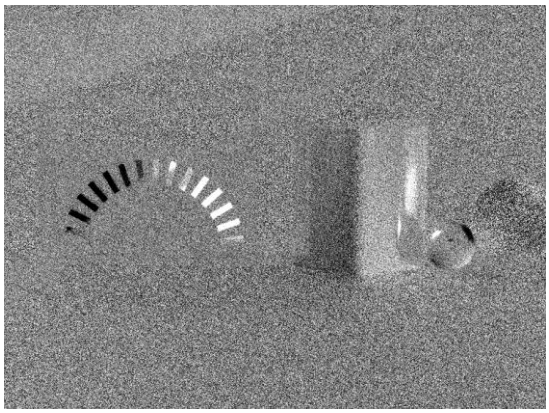

S2

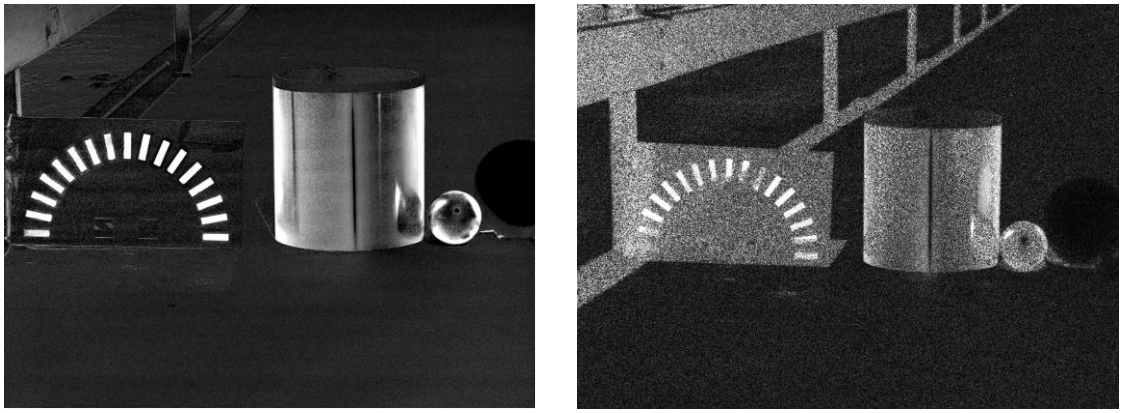

DoLP DoLP

Figure 31. Fluxdata (left) and Salsa (right)

The first comparison begins with Hermann Hall on the campus of the Naval Postgraduate School. The scenes were captured at 1620 PST on September 8, 2016. Both cameras display similar polarization signatures in S1, S2, and DoLP when viewed in their entirety. It is easier to distinguish and identify objects in the Fluxdata. Differences in the cars and windows make them easily visible based on their polarization signature. When zooming in and comparing values of DoLP the Fluxdata gives higher values on objects such as windows and cars. The Salsa loses much of this detail when zooming in on an object. The DoTP of the Salsa is affected by movement and gives false data for moving objects such as trees. Fluxdata's DoAMP is not affected by movement of trees but registration errors do occur from very small errors in the alignment of the frames on the camera in shadows and along some objects outlines. The Fluxdata best displays differences in S1 and S2 to determine which polarization signature is strongest and help classify objects with more accurate data. The DoLP image best portrays the highly-polarized cars on the bottom of the scene. The detail of displaying polarization is seen throughout the data analysis portion of the cameras.

S0

S0

S1

S1

S2

S2

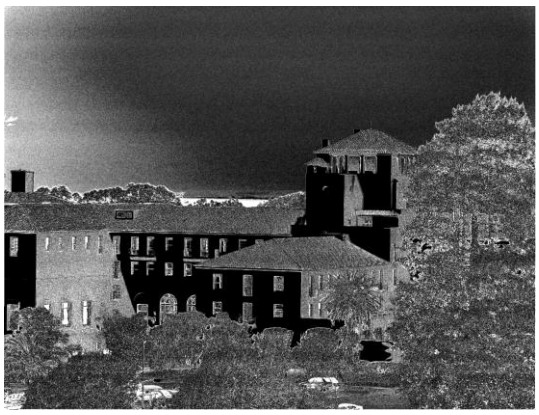

DoLP

DoLP

Figure 32. 8 September, 2016. Hermann Hall, Monterey, CA. Fluxdata(left) Salsa (right)

Figure 33. S0 zoomed in cars Fluxdata (left), Salsa (right)

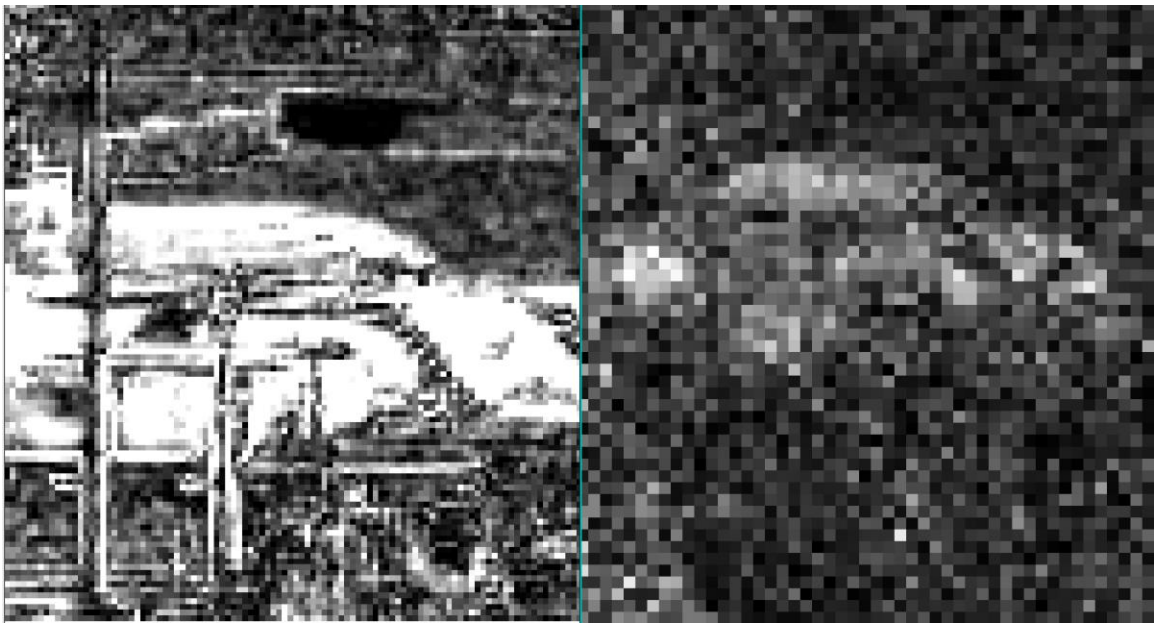

Figure 34. DoLP zoomed in cars Fluxdata (left), Salsa (right)

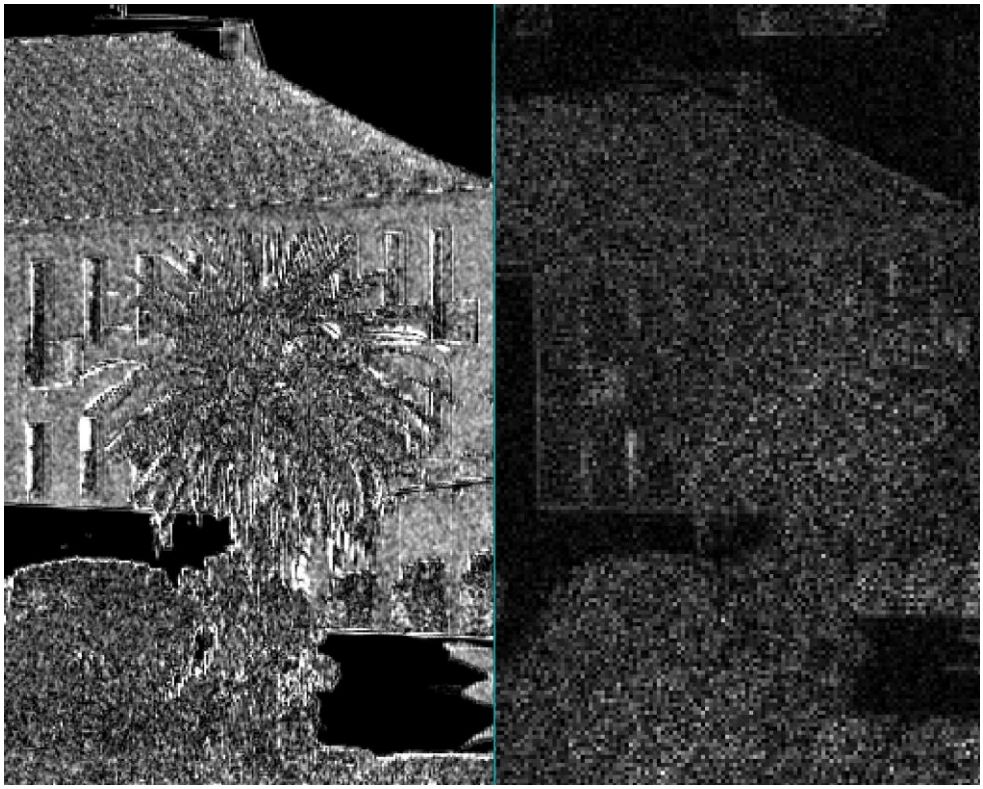

Figure 35. DoLP palm tree zoomed in Fluxdata (left), Salsa (right)

The next data was collected on Decemeber 1, 2016 at 1226 PST on the rooftop of the Marriot Hotel in Monterey, CA. The scene captures a portion of the Monterey harbor and an adjacent building. It is apparent to see the advantage of the Fluxdata's DoAmP technique with the moving seagulls in the top right portion of the Fluxdata. This technique is an advantage over the Salsa because it is not affected by movement which causes registration errors and false data on polarization signatures. Although these images do not portray any major object identification from their polarization, the Fluxdata again captures more detail and is not as affected by the background saturation.

S0

S0

S1

S1

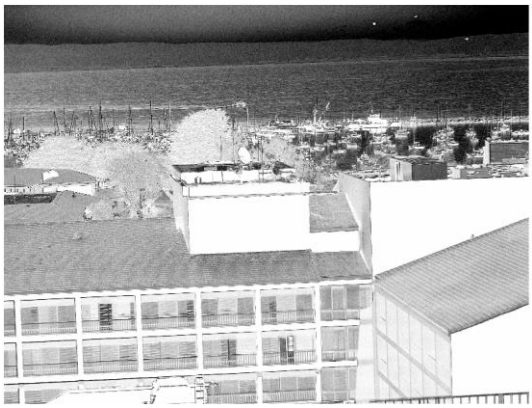

S2

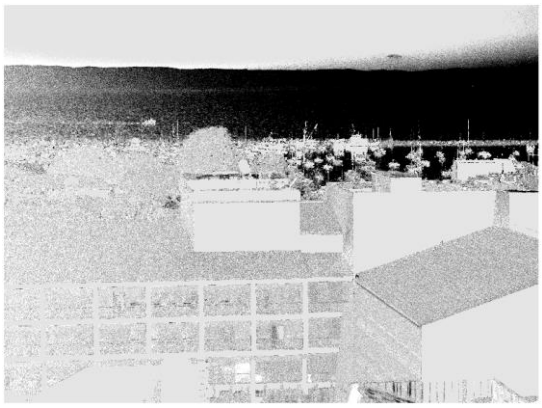

S2

DoLP

DoLP

Figure 36. 1 December, 2016 Marriot rooftop Fluxdata (left), Salsa (right)

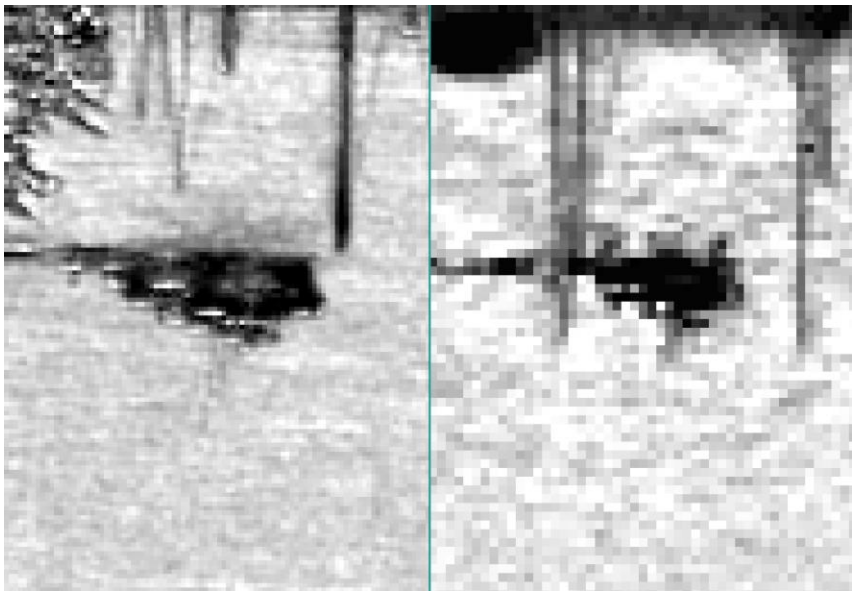

Figure 37. Moving boat on water. Fluxdata (left) Salsa (right)

Figure 38. Seagulls Fluxdata

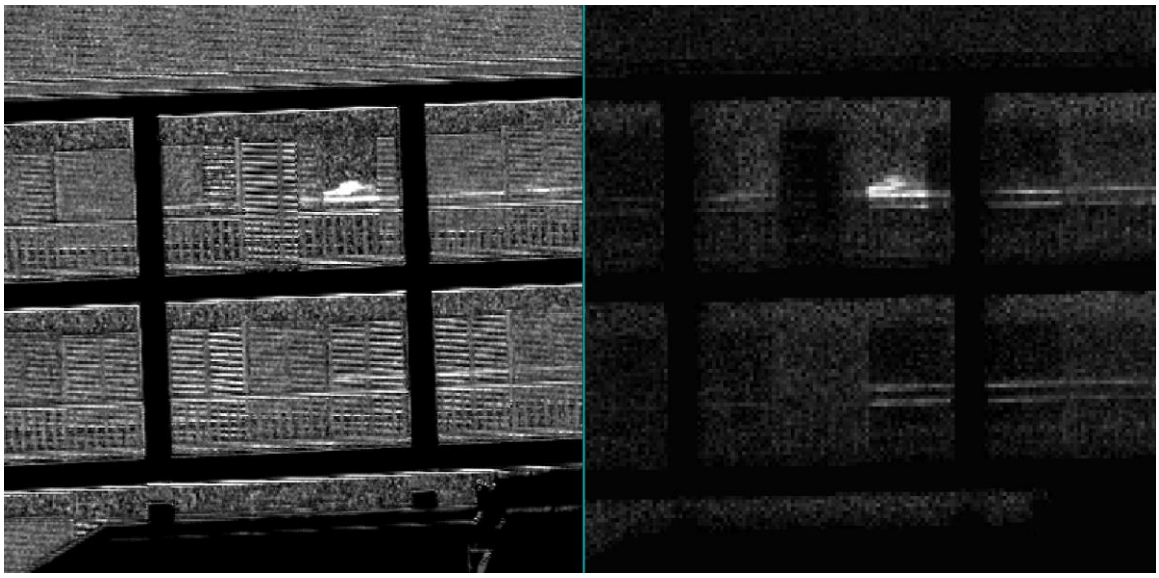

Figure 39. Blinds in windows. Fluxdata (left) Salsa (right)

The next scene was a construction site captured on December 1, 2016 at 1215 PST. The scene had many moving features and items of interest to include wood, metal structures, construction equipment, dirt, gravel, power cables, and people. The Fluxdata's technique of capturing polarization was not affected by the moving aspects of the scene and highly polarized objects such as the windows on a truck and some reflective material on a ledge are distinguishable. The power cable did not show any distinguishable polarization signature and is difficult to detect in any of the Stokes images.

S0

S0

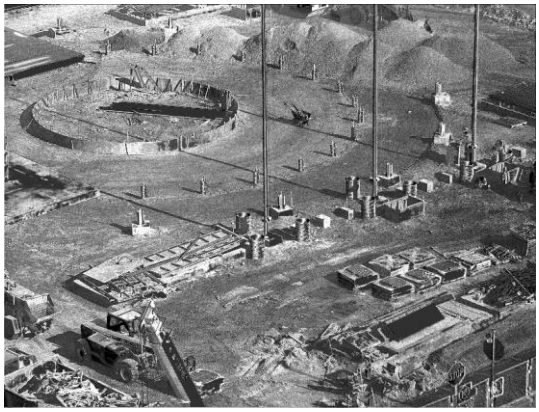

S1

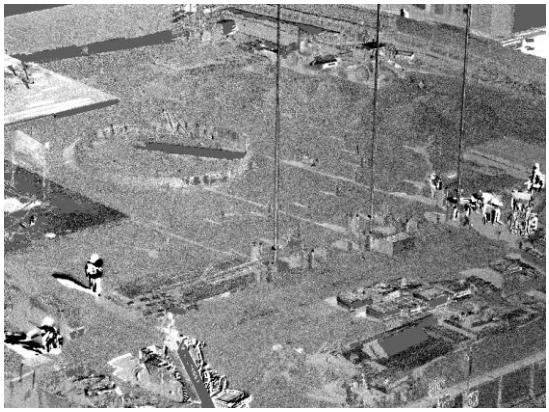

S1

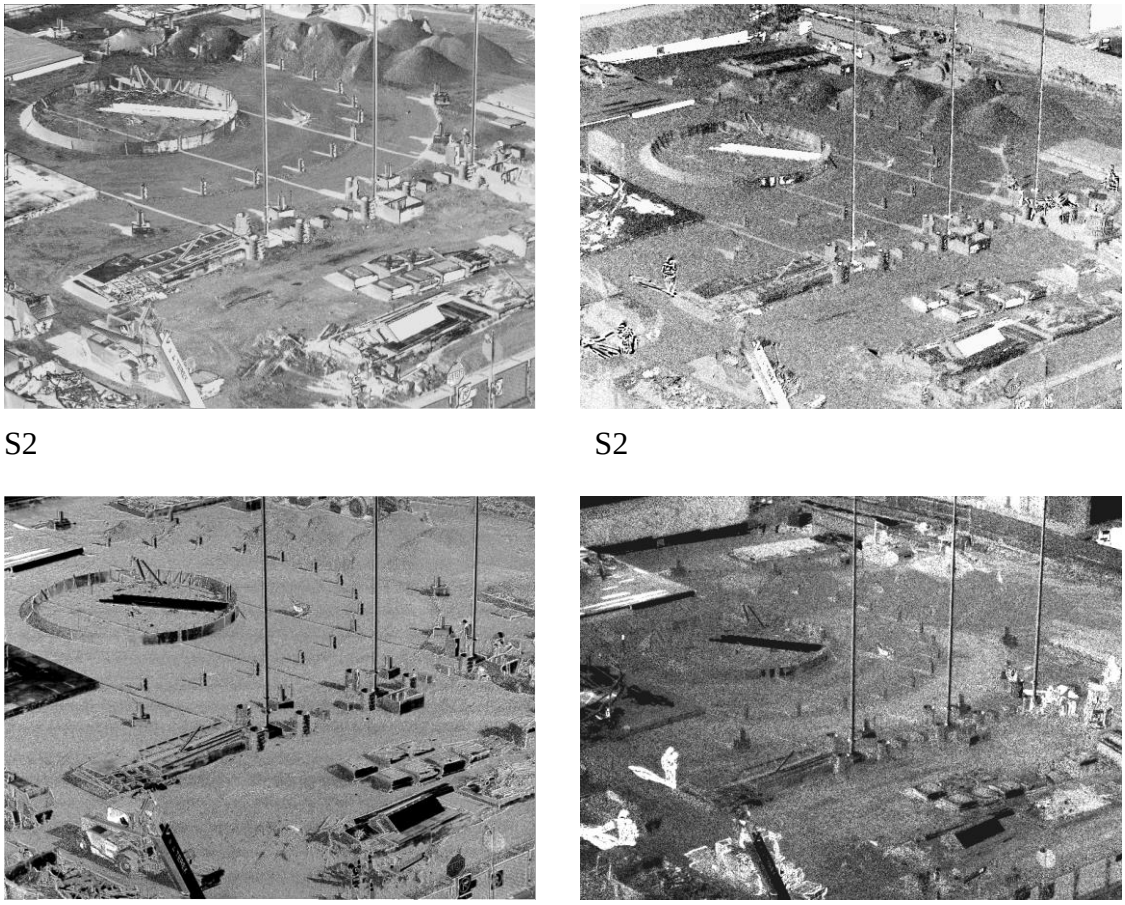

Figure 40. 1 December, 2016. Construction site. Fluxdata (left) Salsa (right)

The remaining analysis focused on the Fluxdata and capturing scenes to expand on potential uses in remote sensing. The Fluxdata's higher resolution and DoAmP display a more accurate pixel calculation of Stokes vectors in moving scenes. For example, trees and their movement are not as affected as they are with the DoTP in the Salsa. In addition to the DoAmP, the Fluxdata captures a color image and the UMOV effect is explored to see how wavelength and color affect polarization for its use in classifying objects.

The scene in Figure 39 consisted of a camouflage covering placed over a car to see how camouflage affects polarization. The cars and their windows all display a high polarization signature but the camouflage masks the signature and lowers the degree of

polarization. Much of the light captured in the imagery appears to be partially polarized. The camouflage's DoLP is lower and closer to the signature of the trees. The ability to hide in plain sight is a polarization technique some fish use to hide in the ocean and shows how camouflage can be used to mask metallic objects. (Brady).

S0

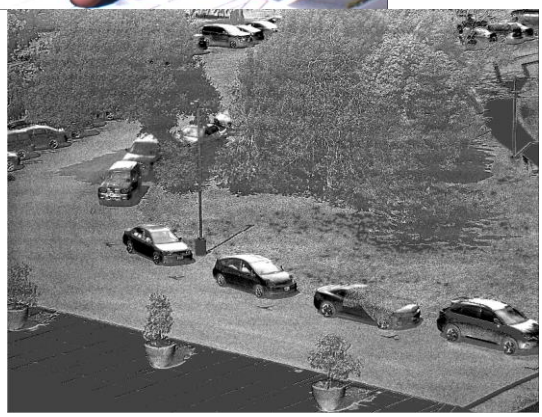

S1

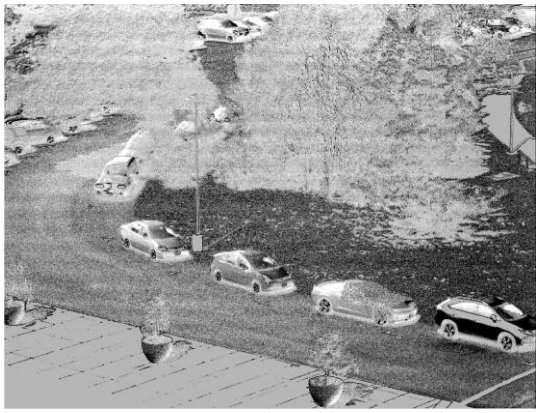

S2

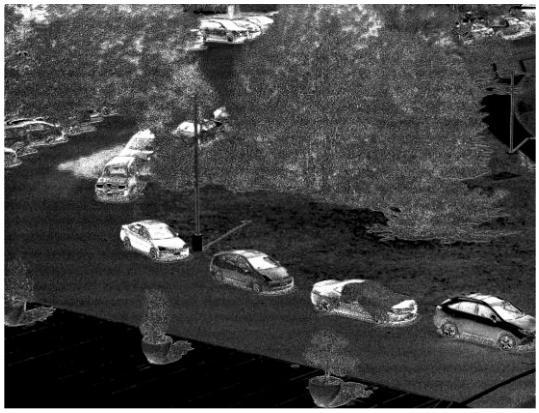

DoLP

Figure 41. 26 September, 2016. Fluxdata camouflage on car scene.

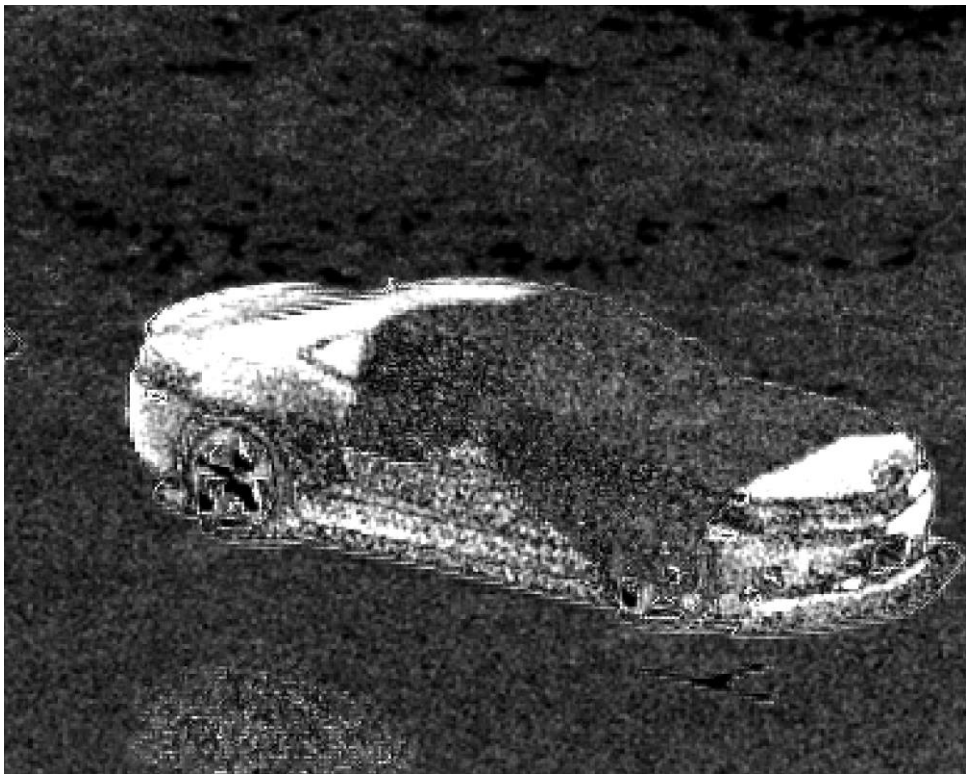

Figure 42. DoLP camoflauge on car

A picture of a magnolia tree and a bare tree was taken at 1154 on 26 September, 2016. The image portrays a mixed degree of small linear polarization signatures and does not contain any major observable artifacts. The small registration errors cause miscalculation's in Stokes.

S0

S1

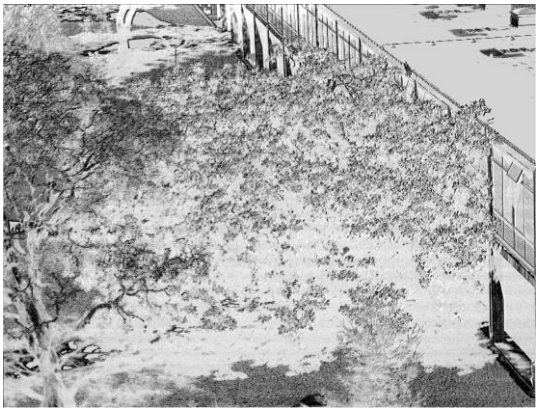

S2

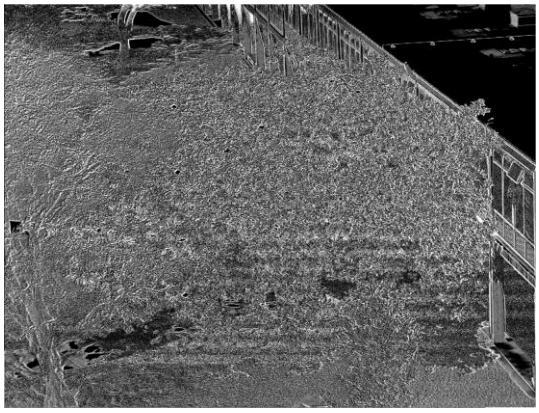

DoLP

Figure 43. 26 September, 2016. Magnolia tree

The scene in Figure 42 was taken on July 8, 2016 at 1527 PST. The scene contains a large vegetation and building combination with a large arrangement of powerlines and wires connecting on top of the building and in the background. The powerlines are more easily viewed in the Stokes and DoLP representations

S0

S1

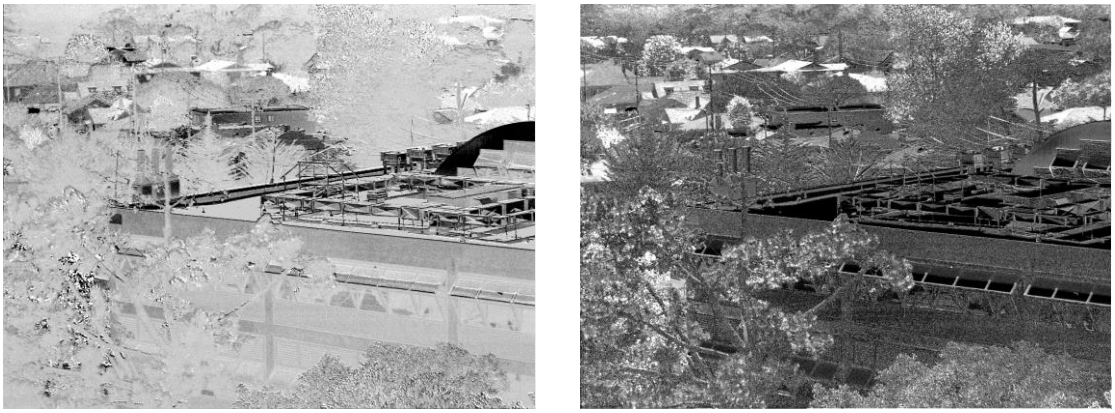

S2 DoLP

Figure 44. 8 July, 2016 Bullard Hall, Monterey, CA

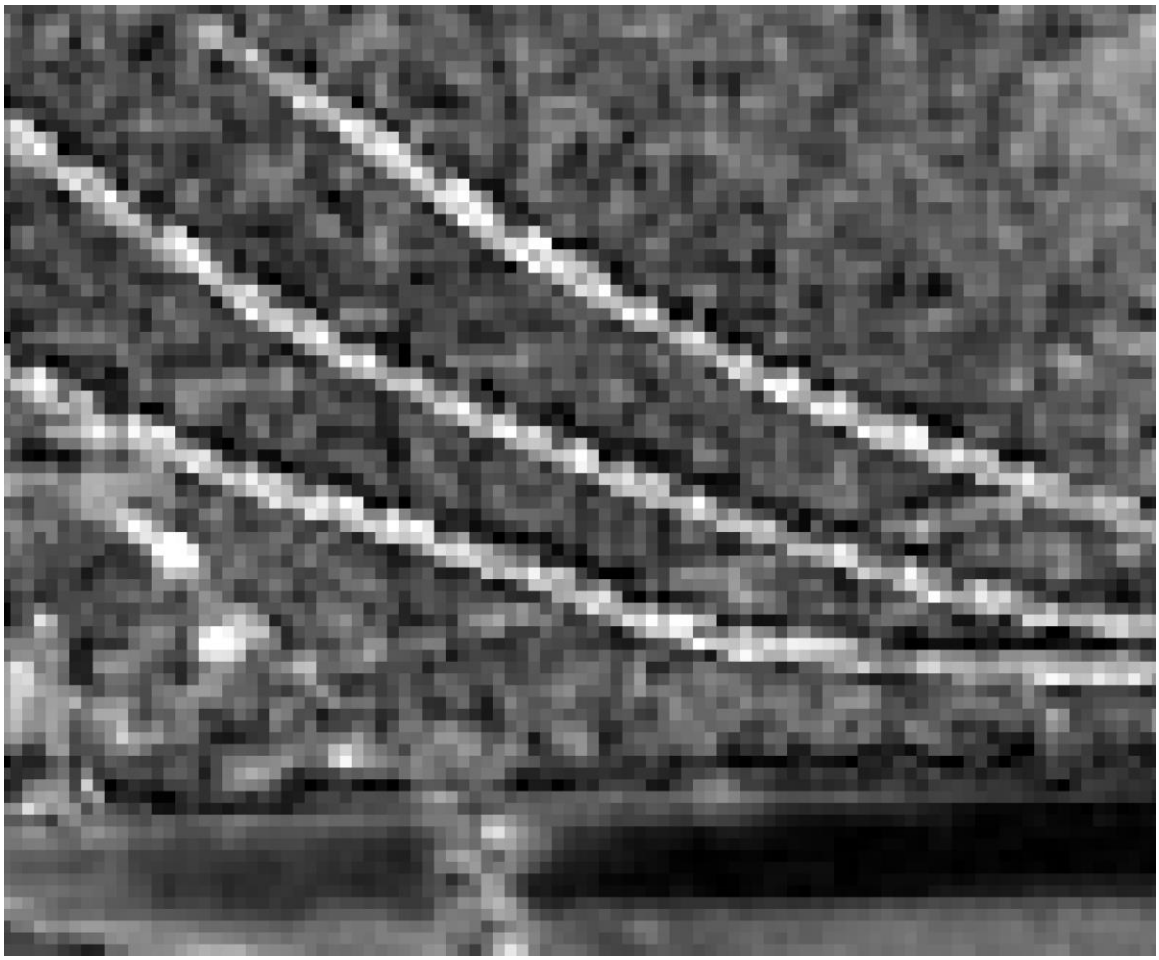

Figure 45. DoLP zoomed in powerlines

The UMOV effect was explored in the construction scene and various other scenes by creating regions of interest in ENVI and comparing their DoLP and Inverse Intensity. The assumption was the Fluxdata's color filters would show the relationships between color, DoLP, and the inverse intensity. There was no conclusive evidence in to display the UMOV effect.

VI. CONCLUSION AND RECOMMENDATIONS

The Salsa and Fluxdata both provide similar polarization representations. The comparison of the imagery confirms polarization signatures and the calculation of correct Stokes vectors and products. The Fluxdata's division of amplitude polarimeter removes the effects of false polarization because of scene movement (Goldstein, p. 389). The advantage of this technique over the Salsa's division of time polarimeter allows the camera to be used on moving vehicles and aircraft because it is not affected by a rotating filter to calculate Stokes. Additionally, the effects of moving trees and objects in a scene can be correctly captured and calculated. The Fluxdata's focal plane alignment causes small registration errors that may need to be adjusted.

A concern in the field of polarization is the lack of data and scenes to be analyzed to determine its best use of polarization for remote sensing. Appendix A includes numerous scenes displaying Stokes images to help expand the library of polarized images for remote sensing. The uses of polarization in remote sensing will continue to grow as more objects and scenes are explored.

The limitations of imaging polarization include sun angle, clouds, saturation, and registration errors. The Fluxdata removes the concern of movement and in future work the DoAmP technique can be used on ground and air vehicle to capture overhead angles to help expand the library of polarization scenes.

The addition of color in polarimetric imaging may be prevalent in target detection and classification based on the wavelength and signature. The UMOV effect has been explored to show a relation in the wavelength with the Fluxdata's color capability. This relationship was not conclusive to display the UMOV effect and needs to be further studied to determine its use in object classification and target detection.

Furthermore, the Fluxdata has the capability to calculate Stokes in real time with software and code implementation. Future work with real time imagery will allow the user to select areas of interest easier and adjust angles to best capture a scene and identify objects.

APPENDIX A. FLUXDATA IMAGES

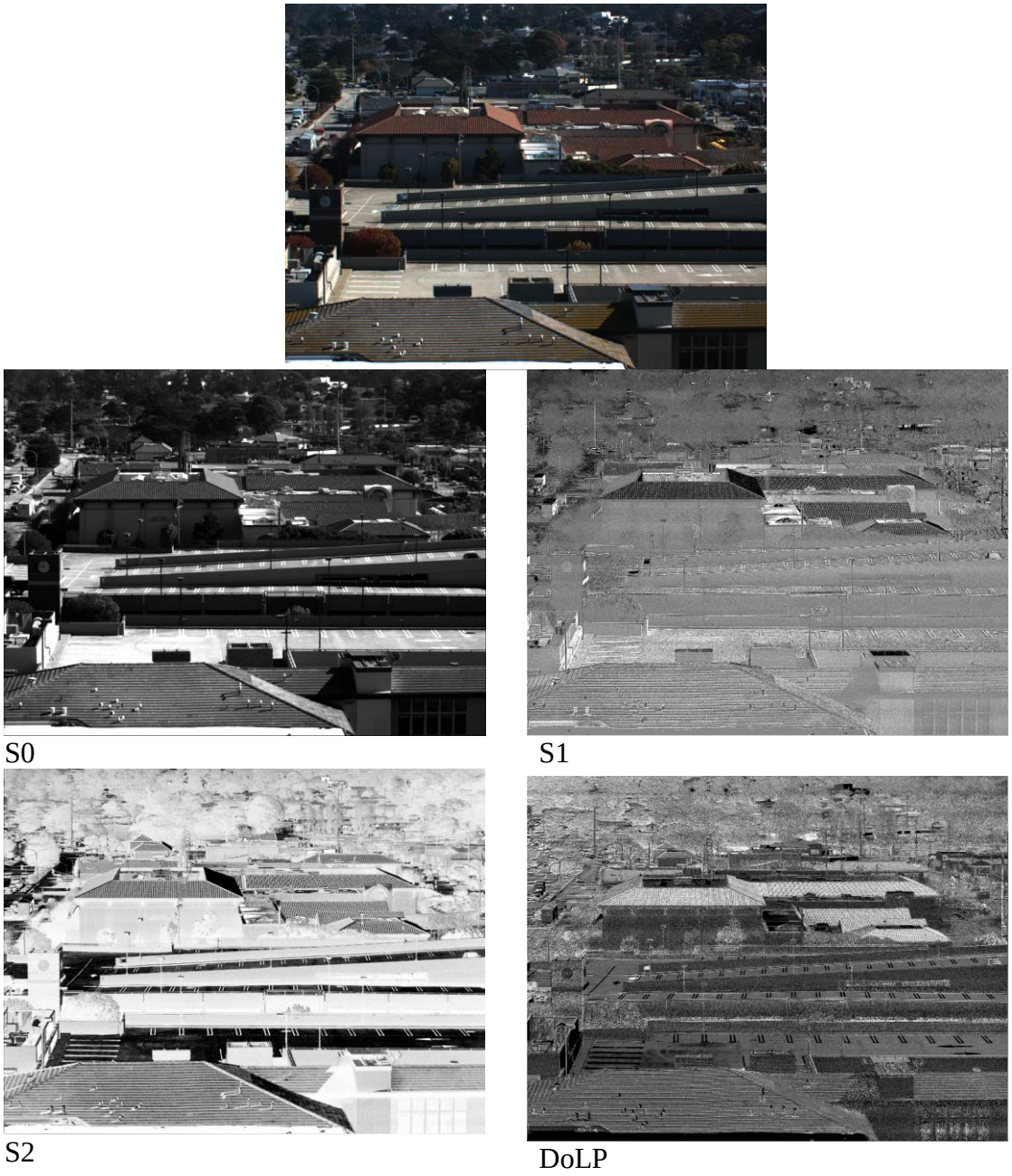

Figure 46. 1147 1 December, 2016

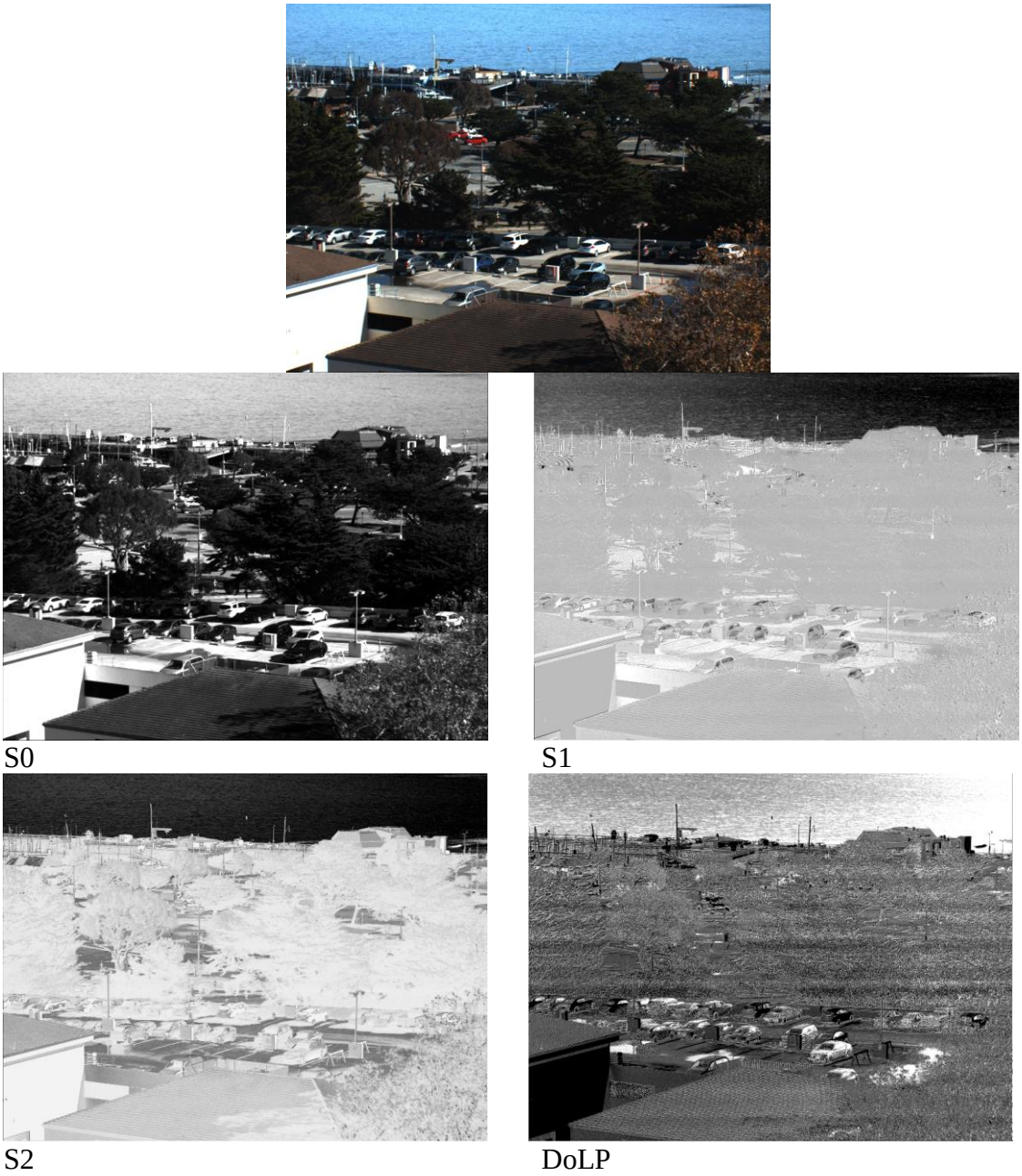

Figure 47. 1200 1 December, 2016

S0

S1

S2

DoLP

Figure 48. 1208 1 December, 2016

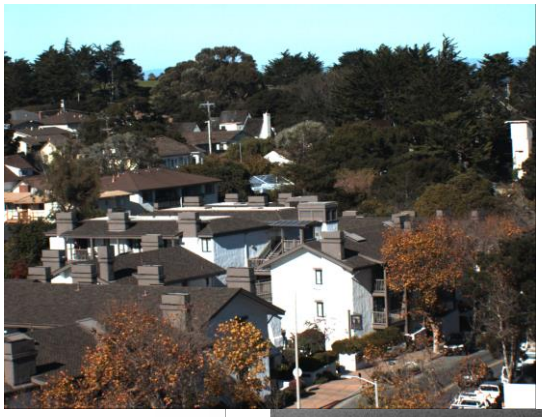

S0

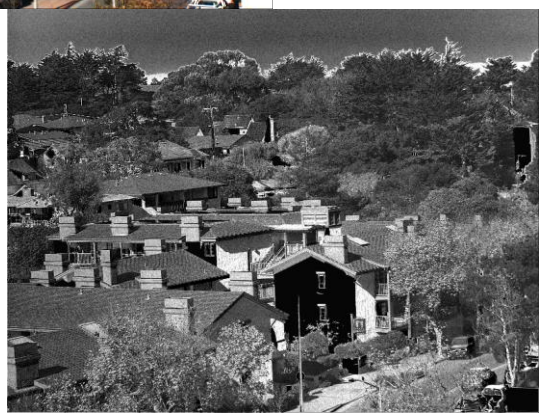

S1

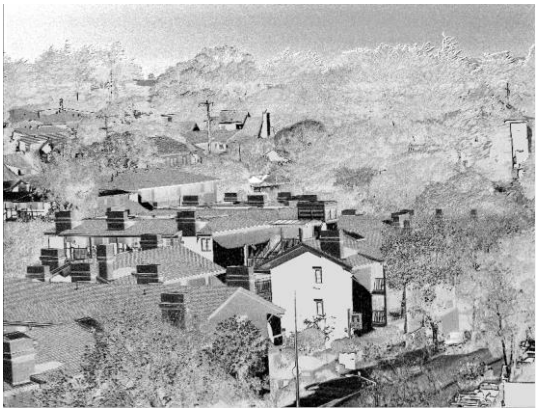

S2

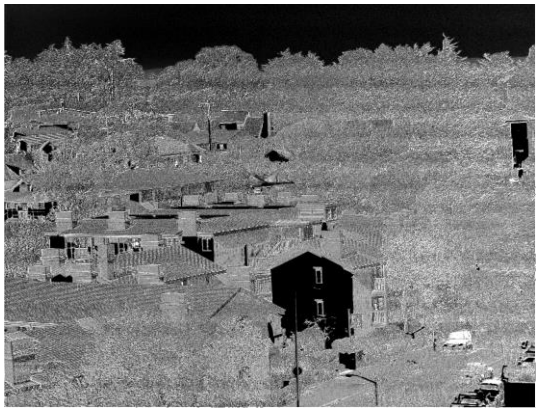

DoLP

Figure 49. 1223 1 December, 2016

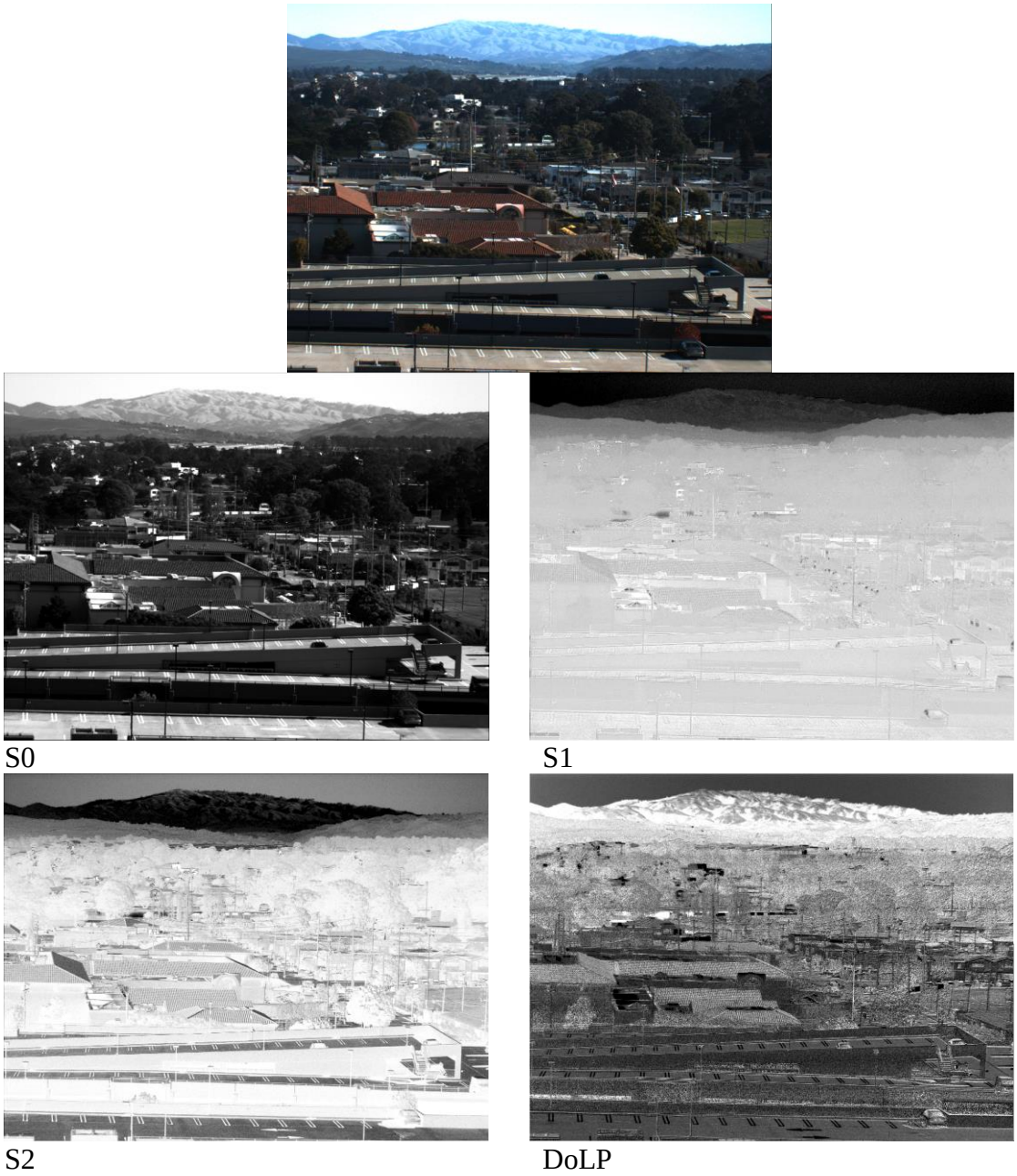

Figure 50. 1237 1 December, 2016

Figure 51. 1242 1 December, 2016

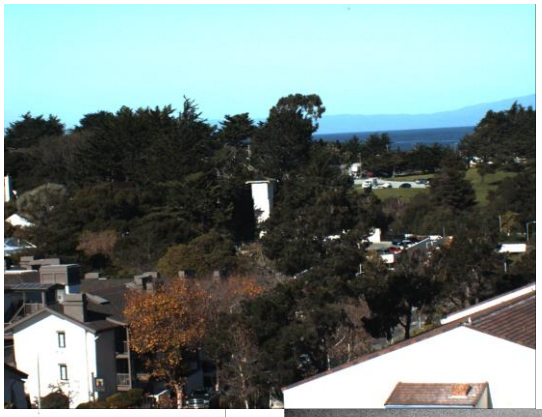

S0

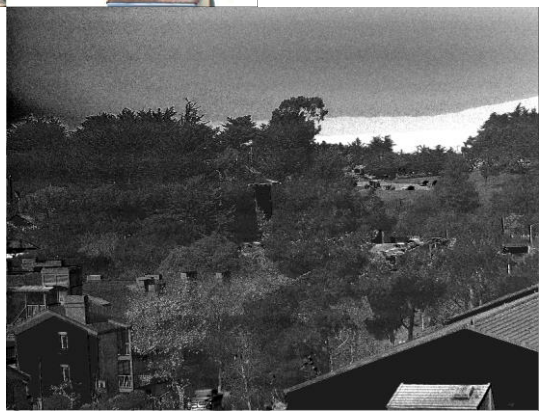

S1

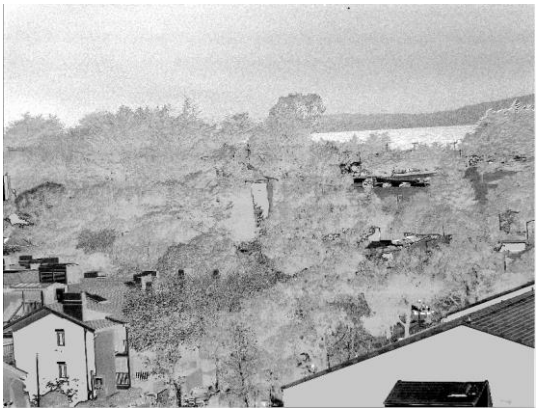

S2

DoLP

Figure 52. 1305 1 December, 2016

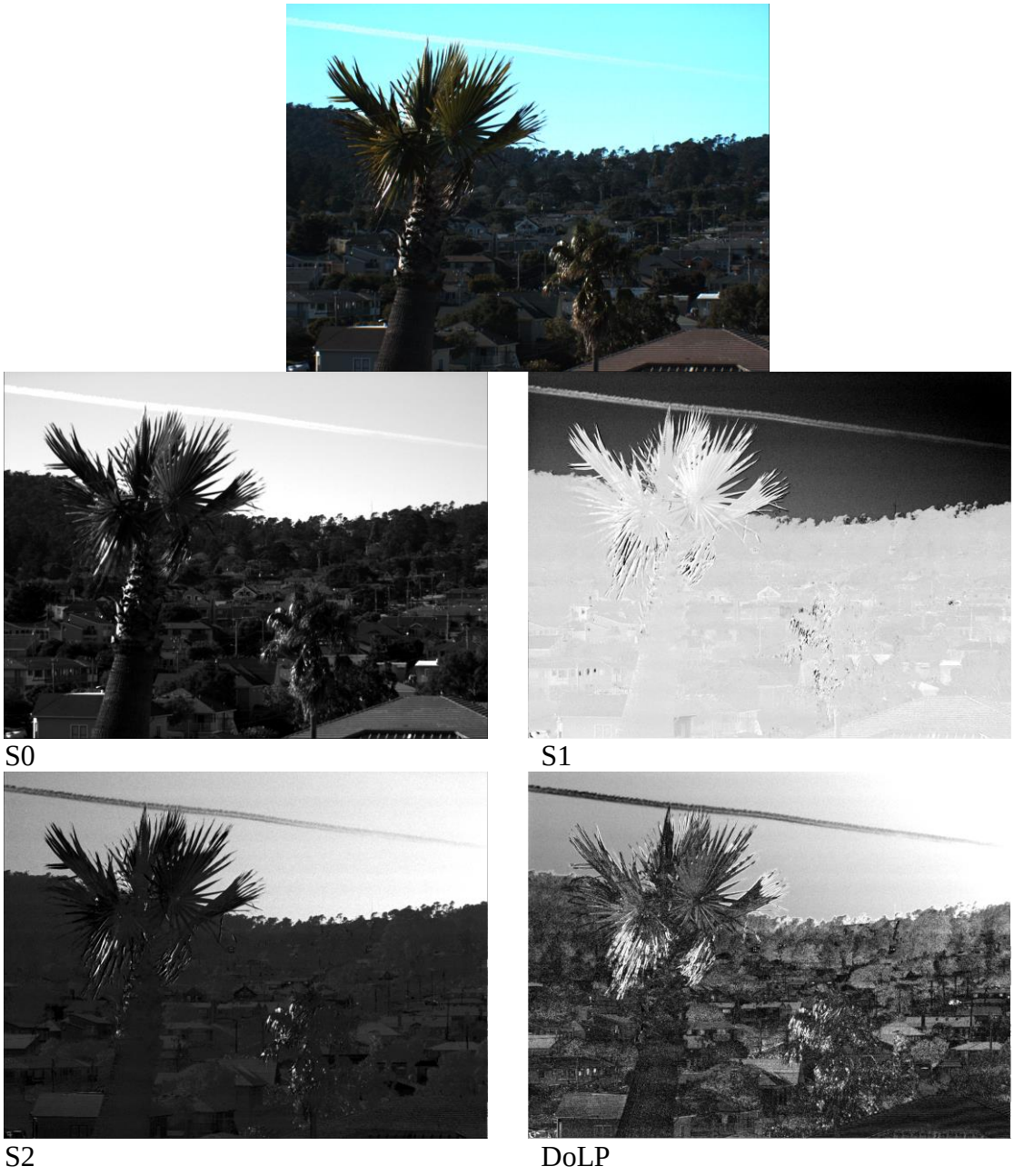

Figure 53. 1312 1 December, 2016

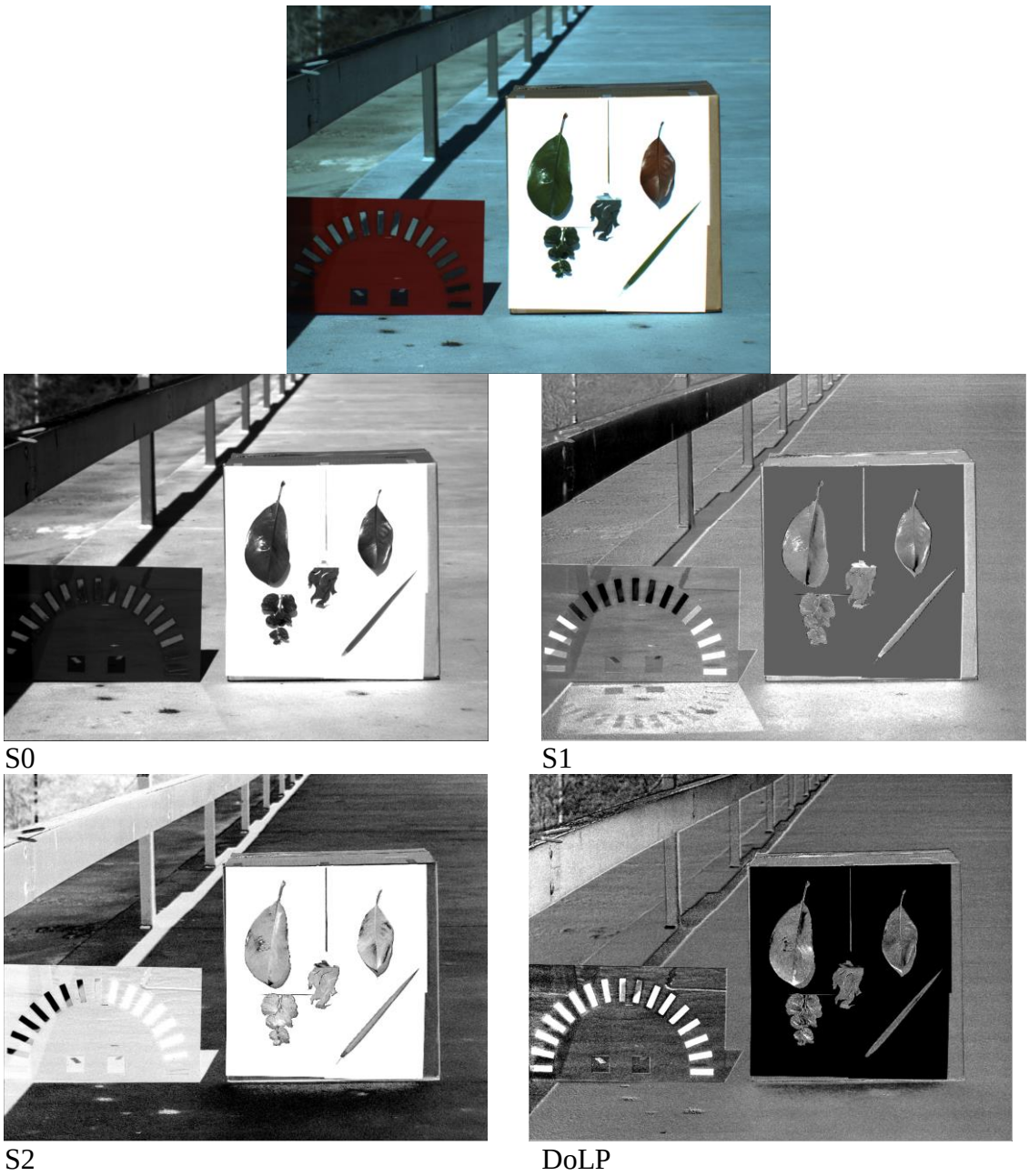

Figure 54. 1238 6 October, 2016

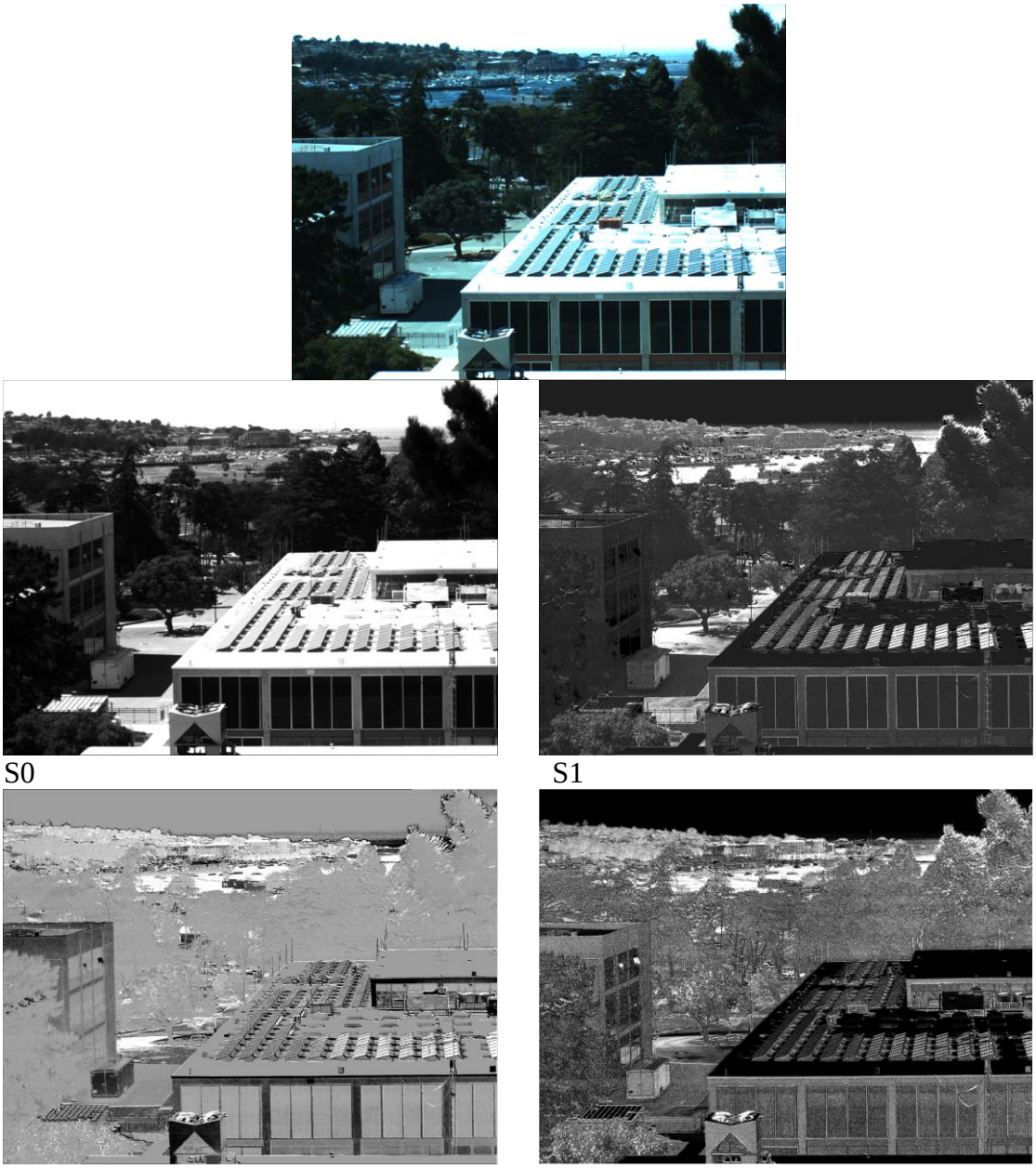

Figure 55. 1529 8 July, 2016

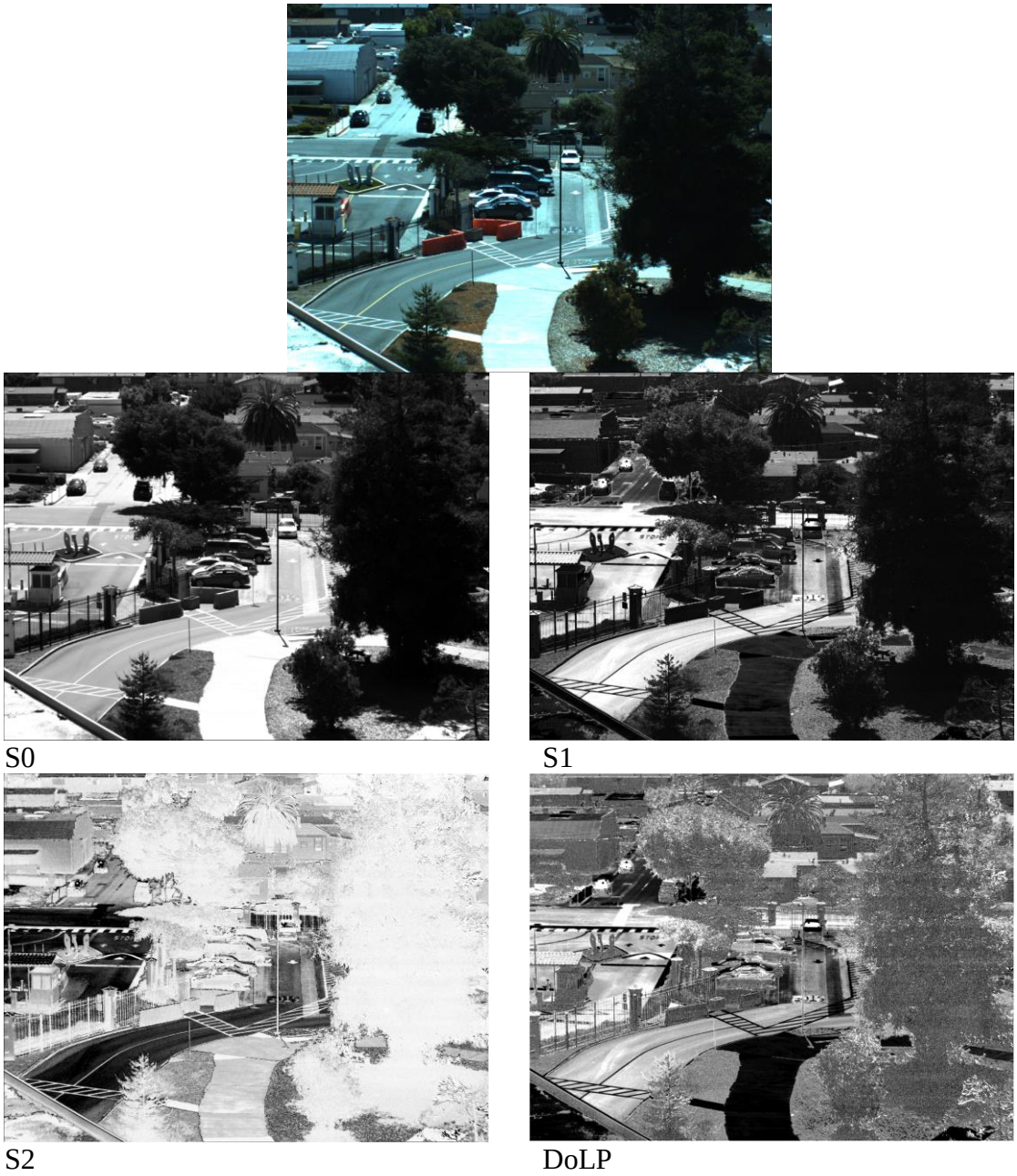

Figure 56. 1520 8 July, 2016

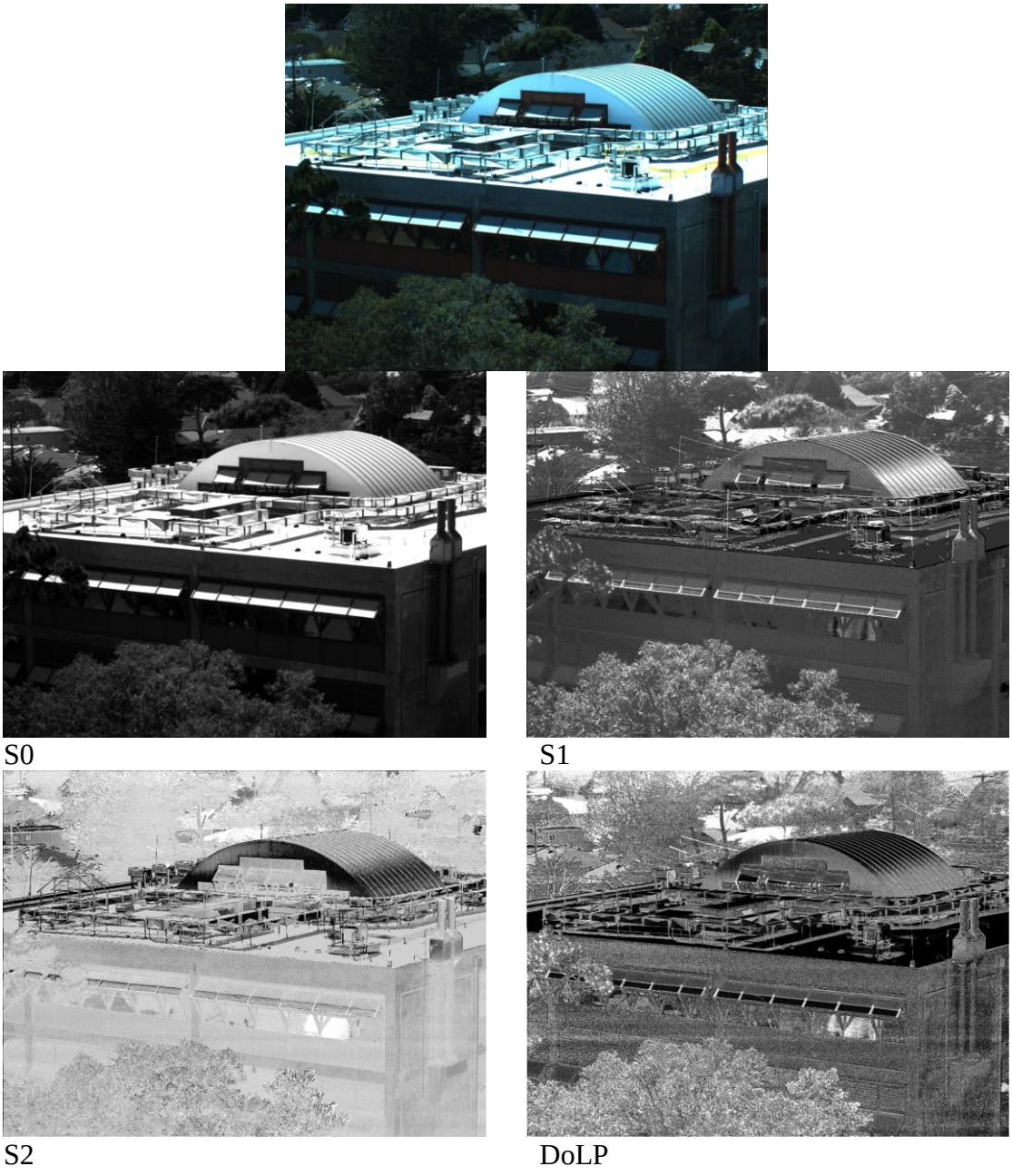

Figure 57. 1532 8 July, 2016 Watkins

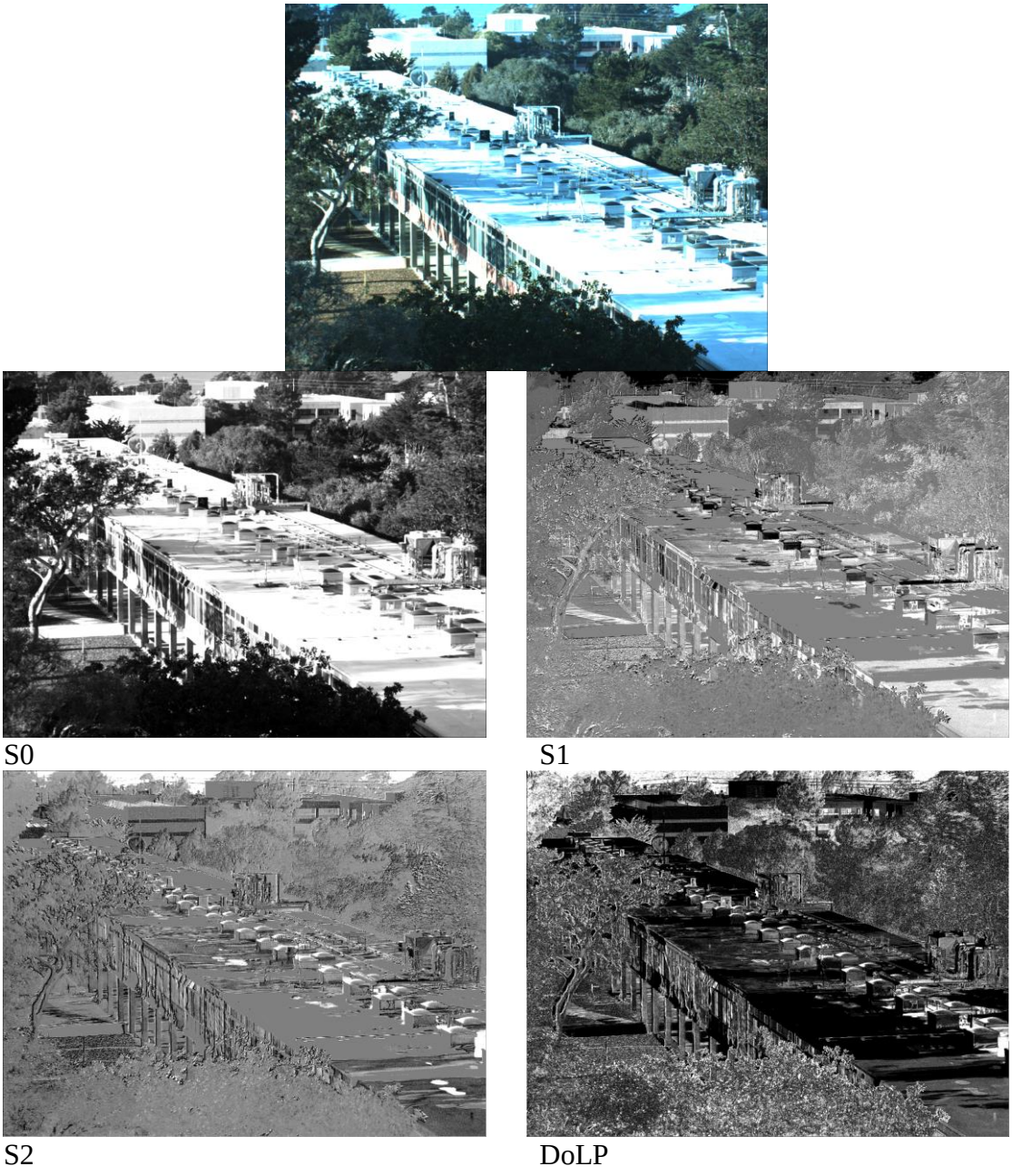

Figure 58. 1535 15 January, 2016 Root Hall

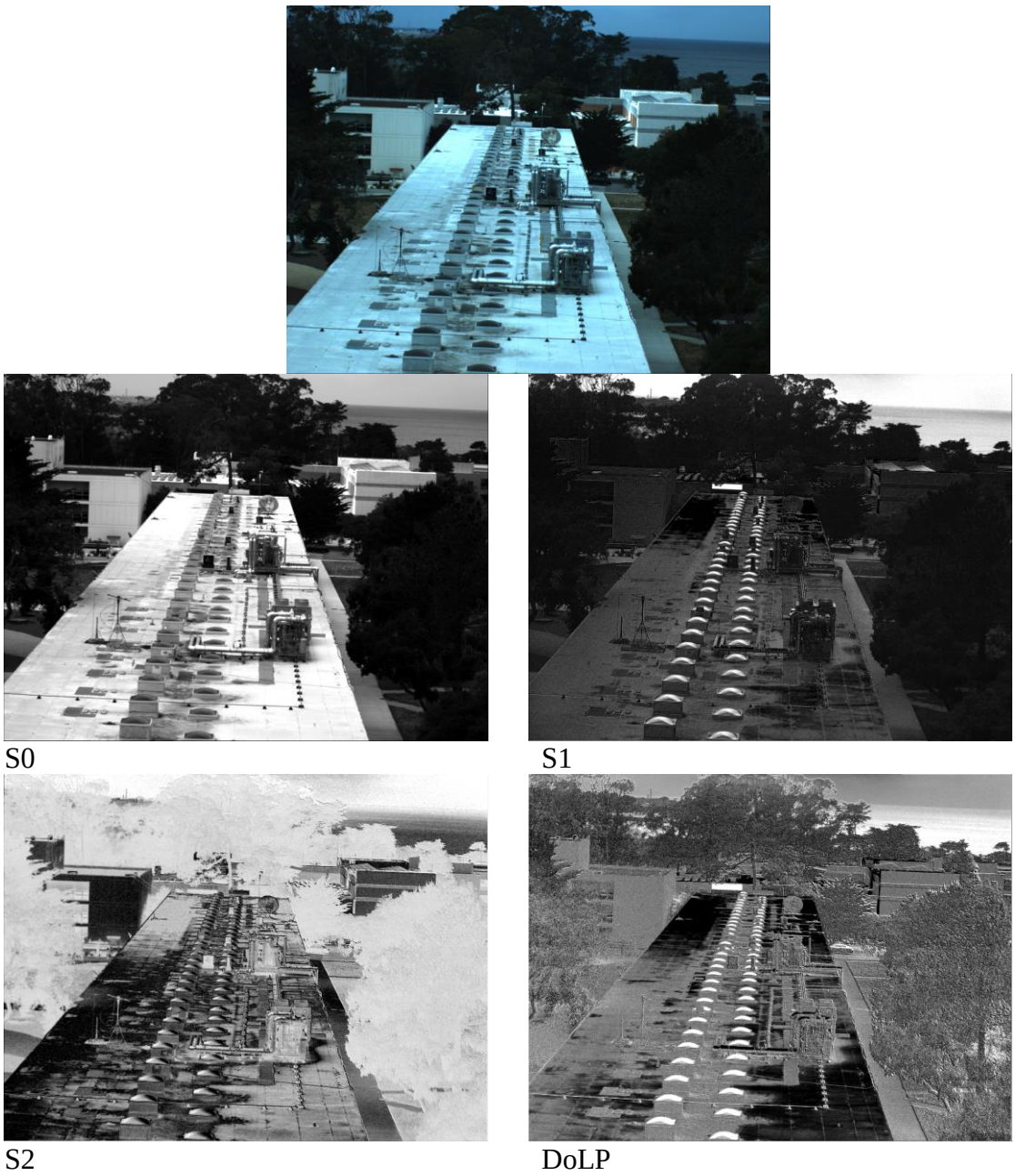

Figure 59. 1425 20 May, 2016

S0

S1

S2

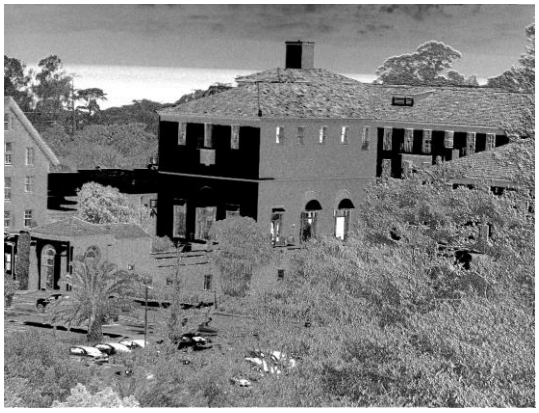

DoLP

Figure 60. 1422 20 May, 2016

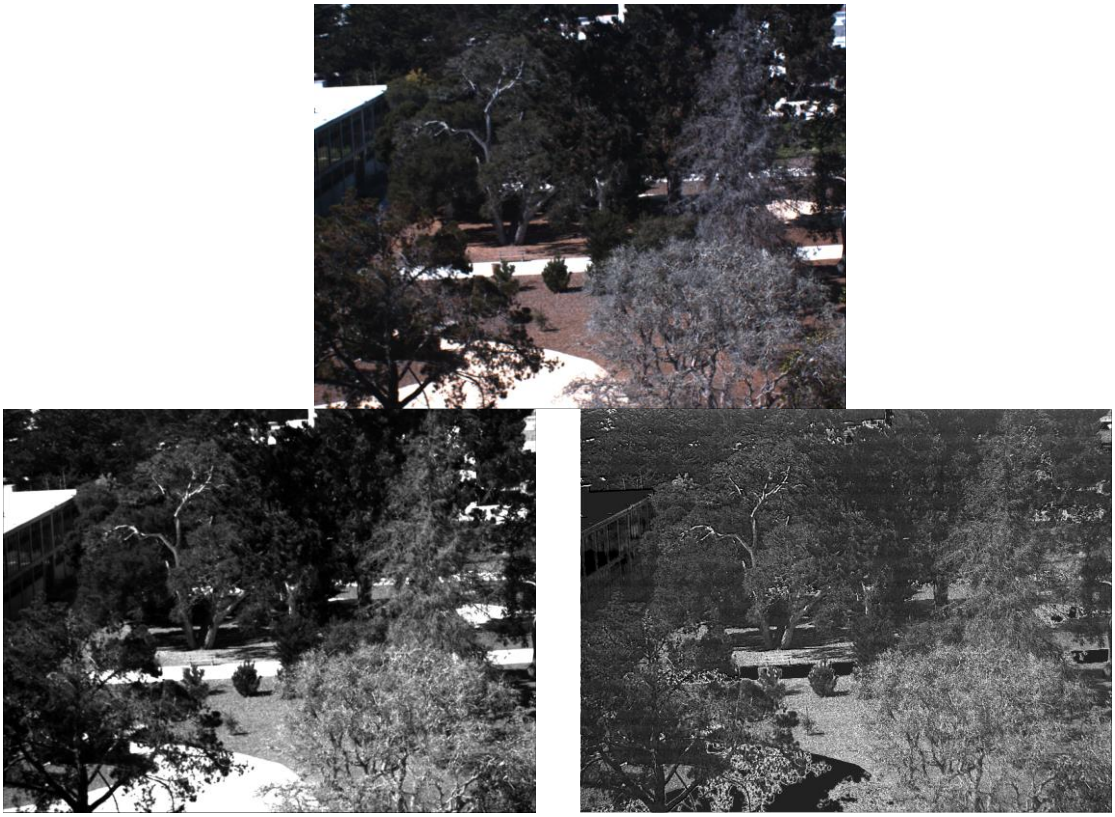

Figure 61. 1420 26 September, 2016

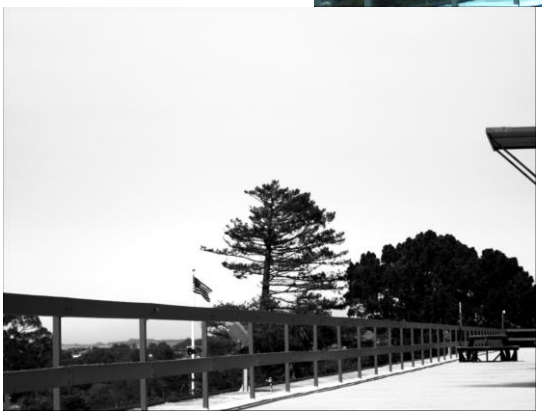

S0

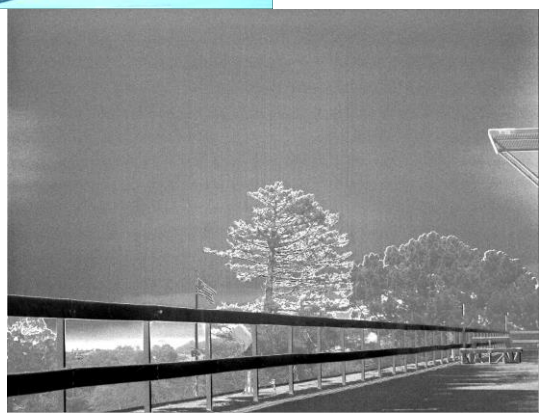

S1

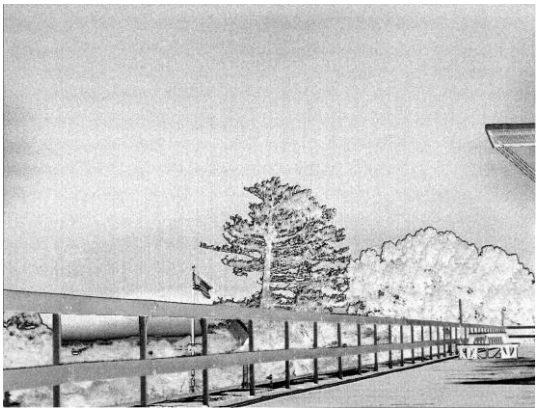

S2

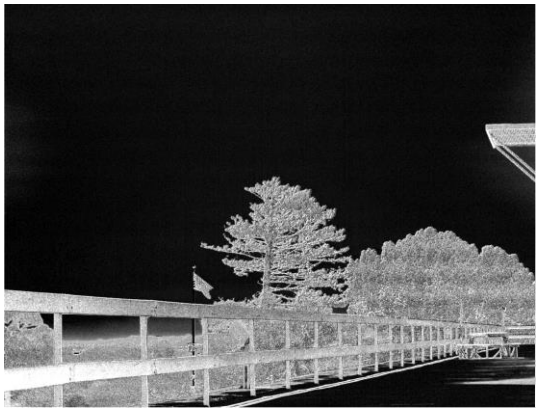

DoLP

Figure 62. 1540 29 July, 2016

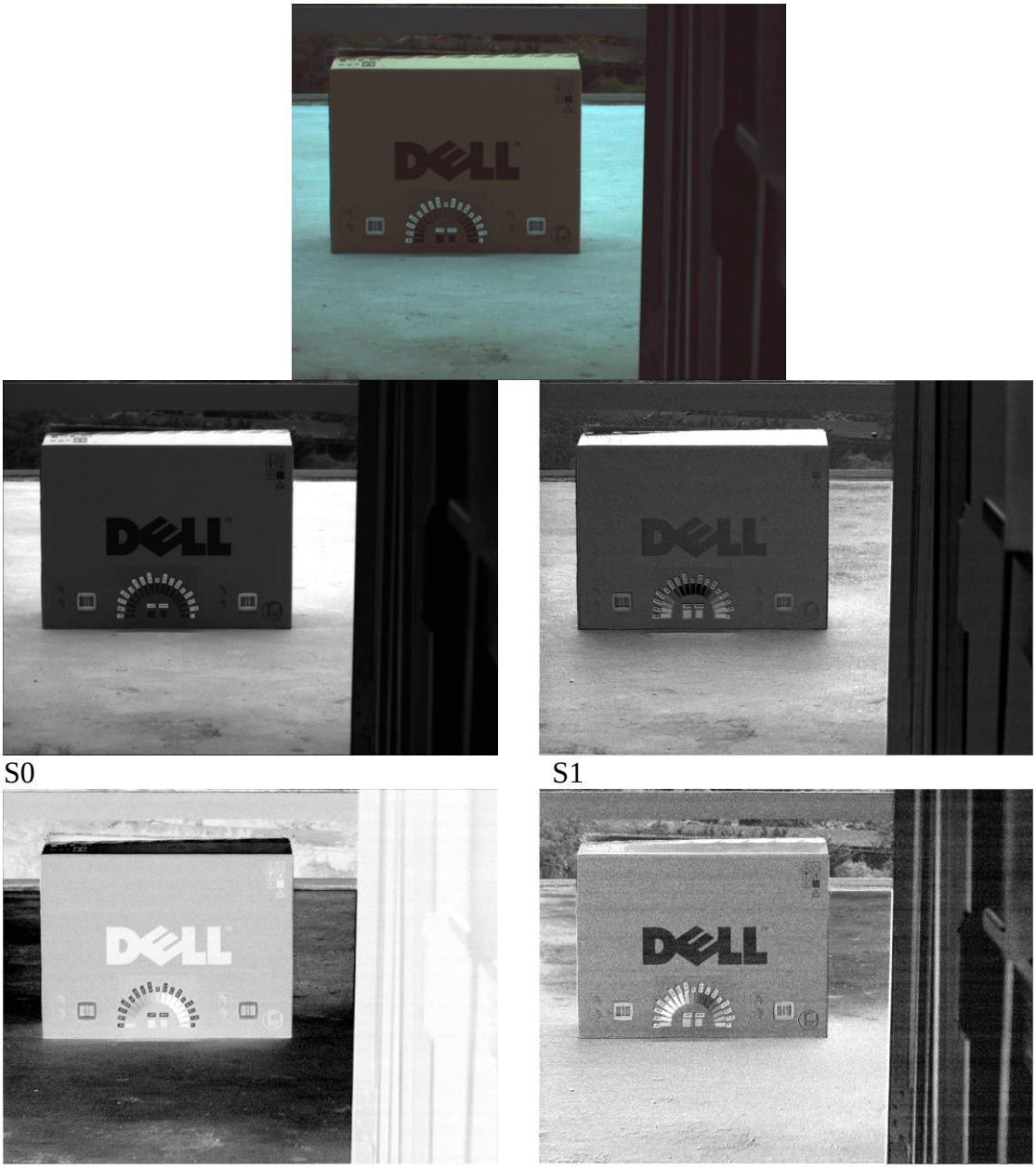

Figure 63. 1552 12 May, 2016

THIS PAGE INTENTIONALLY LEFT BLANK

LIST OF REFERENCES

Azzam, R. M. A., and N. M Bashara. Ellipsometry and Polarized Light (Amsterdam ; New York : New York: North-Holland Pub. Co., 1977).

Bossa Nova Tech. (2007). Polarization imaging SALSA camera applications. Venice, CA: Bossa Nova Technologies.

Bossa Nova Tech. (2007). Salsa linear Stokes polarization imaging - user manual. Venice, CA: Bossa Nova Technologies

Boundless. Boundless Physics. Polarization By Scattering and Reflecting. n.p., 2016. https://www.boundless.com/physics/textbooks/boundless-physics-textbook/wave-optics-26/further-topics-176/polarization-by-scattering-and-reflecting-643-6054/.

Brady, Parrish C. "Scientists discover new camouflage mechanism fish use in open ocean." Phys.org - News and Articles on Science and Technology. November 20, 2015. Accessed February 13, 2017. https://phys.org/news/2015-11-scientists-camouflage-mechanism-fish-ocean.html.

Brosseau, Christian. Fundamentals of Polarized Light: A Statistical Optics Approach (New York: Wiley, 1998).

Chen, H. S., C. R. Nagaraja Rao, Z Sekera, and Air Force Cambridge Research Laboratories (U.S.). Investigations of the Polarization of Light Reflected By Natural Surfaces (Los Angeles: University of California, Dept. of Meteorology, 1976).

Collett, Edward, and Society of Photo-optical Instrumentation Engineers. Field Guide to Polarization (Bellingham, Wash.: SPIE, 2005).

Easton, Robert. "Interaction of Light and Matter." November 29, 2004. Accessed February 13, 2017. https://www.cis.rit.edu/class/simg712-01/notes/basicprinciples-08.pdf.

Eyler, M. (2009). Polarimetric imaging for the detection of disturbed surfaces. Naval Postgraduate School, Monterey: NPS.

Feofilov, P. P. The Physical Basis of Polarized Emission (New York: Consultants Bureau, 1961).

Goldstein, Dennis H., and Edward Collett. Polarized Light (New York: Marcel Dekker, 2003).

Henderson, Thomas. "Polarization." Polarization. Accessed February 09, 2017. http://www.physicsclassroom.com/class/light/Lesson-1/Polarization.

Olsen, R. C. (2015). Remote sensing from air and space. Bellingham, WA: SPIE–The International Society for Optical Engineering

Pappas, Stephanie. "How Do We See Color?" LiveScience. April 29, 2010. Accessed February 09, 2017. http://www.livescience.com/32559-why-do-we-see-in-color.html.

Robinson, Philip C. "Polarized Light Microscopy." Nikon's MicroscopyU. Accessed February 09, 2017. https://www.microscopyu.com/techniques/polarized-light/polarized-light-microscopy.

Schott, Brosseau, Christian. Fundamentals of Polarized Light: A Statistical Optics Approach (New York: Wiley, 1998).

Shell, James R. Polarimetric Remote Sensing in the Visible to Near Infrared. Rochester Institute of Technology. Rochester, NY

Smith, P. (2008). The uses of a polarimetric camera. Naval Postgraduate School, Monterey: NPS.

Smith, Randall B. Introduction to interpreting digital RADAR images. January, 4, 2012. http://www.microimages.com/documentation/Tutorials/radar.pdf.

Swindell, William. Polarized Light (Stroudsburg, Pa. : [New York]: Dowden, Hutchinson & Ross, 1975).

Tyo, S, "Polarization difference imaging: A means for seeing through scattering media" (January 1, 1997).

Tyo, S., et al. (1995, March). Polarization-difference imaging: A biologically inspired technique for observation through scattering media. Optics Letters, 20(6), 608610.

Tyo, S., et al. (1996, April). Target detection on optical scattering media by polarization difference imaging. Applied Optics, 35(11), 1855-1870.

Tyo, S., et al. (1998, February). Colormetric representation for use with polarizationdifference imagery in scattering media. Journal of Optical Scientists of America, 15(2), 367-374.

Tyo, S., et al. (2006, August 1). Review of passive imaging polarimerty for remote sensing application. Applied Optics 45(22), 5453-5469.

Umansky, M. A Prototype Polarimetric Camera for Unmanned Ground Vehicles. Virginia Polytechnic Institute and State University.

West, D. (2010). Disturbance detection in snow using polarimetric imagery of the visible spectrum. Naval Postgraduate School, Monterey: NPS.

Zubko, Evgenij, Gorden Videen, Yuriy Shkuratov, Karri Muinonen, and Tetsuo Yamamoto. "The Umov effect for single irregularly shaped particles with sizes comparable with wavelength." Icarus 212, no. 1 (2011): 403-15. doi:10.1016/j.icarus.2010.12.012.

NOAA. "Dual Polarized Radar." NOAA National Severe Storms Laboratory. Accessed February 17, 2017. http://www.nssl.noaa.gov/tools/radar/dualpol/.

Lou, Yunling The Nasa/JPL Airborne Synthetic Aperture Radar System. Accessed February 17, 2017. https://airsar.jpl.nasa.gov/documents/genairsar/airsar_paper1.pdf/.

THIS PAGE INTENTIONALLY LEFT BLANK

DTIC and DKL are the **only** two entities that are to appear on this page.

Include your desired recipients in your Publication Announcement List form. Thesis forms.

INITIAL DISTRIBUTION LIST

1. Defense Technical Information Center
   Ft. Belvoir, Virginia

2. Dudley Knox Library
   Naval Postgraduate School
   Monterey, California